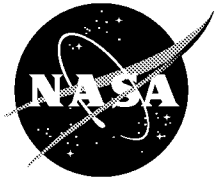# Technical Report Series on the Boreal Ecosystem-Atmosphere Study (BOREAS)

Forrest G. Hall and K. Huemmrich, Editors

Volume 208

BOREAS TF-10 NSA-YJP Tower Flux, Meteorological, and Porometry Data

J. Harry McCaughey and Laura Liblik
Queen's University, Kingston, Ontario

National Aeronautics and
Space Administration

Goddard Space Flight Center
Greenbelt, Maryland 20771

November 2000

The NASA STI Program Office ... in Profile

Since its founding, NASA has been dedicated to the advancement of aeronautics and space science. The NASA Scientific and Technical Information (STI) Program Office plays a key part in helping NASA maintain this important role.

The NASA STI Program Office is operated by Langley Research Center, the lead center for NASA's scientific and technical information. The NASA STI Program Office provides access to the NASA STI Database, the largest collection of aeronautical and space science STI in the world. The Program Office is also NASA's institutional mechanism for disseminating the results of its research and development activities. These results are published by NASA in the NASA STI Report Series, which includes the following report types:
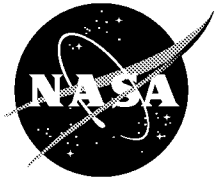
- TECHNICAL PUBLICATION. Reports of completed research or a major significant phase of research that present the results of NASA programs and include extensive data or theoretical analysis. Includes compilations of significant scientific and technical data and information deemed to be of continuing reference value. NASA's counterpart of peer-reviewed formal professional papers but has less stringent limitations on manuscript length and extent of graphic presentations.

- TECHNICAL MEMORANDUM. Scientific and technical findings that are preliminary or of specialized interest, e.g., quick release reports, working papers, and bibliographies that contain minimal annotation. Does not contain extensive analysis.

- CONTRACTOR REPORT. Scientific and technical findings by NASA-sponsored contractors and grantees.

- CONFERENCE PUBLICATION. Collected papers from scientific and technical conferences, symposia, seminars, or other meetings sponsored or cosponsored by NASA.

- SPECIAL PUBLICATION. Scientific, technical, or historical information from NASA programs, projects, and mission, often concerned with subjects having substantial public interest.

- TECHNICAL TRANSLATION. English-language translations of foreign scientific and technical material pertinent to NASA's mission.

Specialized services that complement the STI Program Office's diverse offerings include creating custom thesauri, building customized databases, organizing and publishing research results ... even providing videos.

For more information about the NASA STI Program Office, see the following:

- Access the NASA STI Program Home Page at http://www.sti.nasa.gov/STI-homepage.html

- E-mail your question via the Internet to help@sti.nasa.gov

- Fax your question to the NASA Access Help Desk at (301) 621-0134

- Telephone the NASA Access Help Desk at (301) 621-0390

- Write to:
  NASA Access Help Desk
  NASA Center for AeroSpace Information
  7121 Standard Drive
  Hanover, MD 21076-1320

Technical Report Series on the Boreal Ecosystem-Atmosphere Study (BOREAS)

Forrest G. Hall and K. Huemmrich, Editors

Volume 208

BOREAS TF-10 NSA-YJP Tower Flux, Meteorological, and Porometry Data

J. Harry McCaughey and Laura Liblik
Queen's University, Kingston, Ontario

November 2000

Available from:

BOREAS TF-10 NSA-YJP Tower Flux, Meteorological, and Porometry Data

J. Harry McCaughey, Laura Liblik

Summary

The BOREAS TF-10 team collected tower flux and meteorological data at two sites, a fen and a young jack pine forest, near Thompson, Manitoba, Canada, as part of BOREAS. A preliminary data set was assembled in August 1993 while field testing the instrument packages, and at both sites data were collected from 15-Aug to 31-Aug. The main experimental period was in 1994, when continuous data were collected from the young jack pine site from 23-May to 20-Sep. Upon examination of the 1994 data set, it became clear that the behavior of the heat, water, and carbon dioxide fluxes throughout the whole growing season was an important scientific question, and that the 1994 data record was not sufficiently long to capture the character of the seasonal behavior of the fluxes. Thus, the young jack pine site was operated from 08-May to 07-Nov in 1996 in order to collect data from spring melt to autumn freeze-up. All variables are presented as 30-minute averages. Supporting data were also collected to describe the surface's state and to provide the information, in association with the flux data, to build SVAT models. For the young jack pine site, these supporting data included stomatal conductance measurements. The data are stored in tabular ASCII files.

Table of Contents

1. Data Set Overview

1.1 Data Set Identification
BOREAS TF-10 NSA-OJP Tower Flux, Meteorological, and Porometry Data

1.2 Data Set Introduction
The meteorological data collected from the fen and Young Jack Pine (YJP) towers represent, in some sense, polar opposites of the range of surface climate conditions expected in the boreal forest. The fen is normally characterized by abundant water close to, or located at, the surface, whereas the YJP site can be one of the driest surfaces in the boreal forest. Jack pine generally inhabit well-drained, sandy soils where, in the absence of regular precipitation, a significant water deficit can develop. The data presented here bear out the contrast in the surface climate conditions experienced by the two sites. For example, in the driest periods in the summer of 1994 it was common to measure mid-afternoon Bowen ratios in the range of 10 to 15, leading to the characterization of the site as a "Green Desert"; at the same time, the typical Bowen ratio at the fen seldom exceeded 1.0, and was usually closer to 0.8.

The YJP site can be fairly described as a fast response surface in that there were major and rapid changes in flux behavior, especially in evaporation, as the site was wetted or when it dried down. No such behavior could be ascribed to the fen because of the steadier supply of surface water.

1.3 Objective/Purpose
This project is concerned with the spatial heterogeneity of surface energy fluxes in the northern boreal forest. The study was designed to compare surface radiation, energy, water, CO_2 fluxes, and their biophysical controls at both wetland and upland forest sites within the northern boreal forest. Specific objectives of the study were as follows:
- To quantify the differences between surface-atmosphere interactions between the sites.
- To compare hydrological estimates of basin evaporation to modeled water loss values (computed from knowledge of the vegetational composition of homogeneous landscape units and their ecotones, and the functional response of these units to climatic forcing.
- To provide continuous tower fluxes of water, sensible heat, and CO_2 in support of the development of Soil-Vegetation-Atmosphere-Transfer (SVAT) models at the stand and regional scales.

Data for this study were collected at two sites in the BOReal Ecosystem-Atmosphere Study (BOREAS) Northern Study Area (NSA) at Thompson, Manitoba: a young jack pine forest (YJP), and a fen wetland.

1.4 Summary of Parameters
The following micrometeorological variables were measured at the YJP site: net radiation, incoming and reflected solar radiation, incoming and outgoing longwave radiation, incoming and reflected photosynthetic photon flux density (PPFD), wind speed, wind direction, wet- and dry-bulb temperature, biomass temperature, soil temperature, soil heat flux, sensible heat flux, latent heat flux, CO_2 flux, rainfall, and soil moisture.

In addition, the following biophysical variables were measured: stomatal conductance, leaf temperature, leaf area index (LAI), tree height (h), diameter at breast height (dbh), and tree stem density.

1.5 Discussion
Data collected for this study can be divided into two primary groups: micrometeorological measurements and biophysical measurements.

Micrometeorological Measurements:
The primary objective of this project was to develop a full suite of radiation, energy, and CO_2 flux measurements for the two flux tower sites. At both towers, identical instrumentation was used for data collection. The measurement systems used can be briefly summarized as follows:
- Radiation balance fluxes, including PPFD, were monitored using standard instrumentation mounted near the top of the flux towers.
- Soil heat flux (G) was measured using soil heat flux plates combined with calorimetric calculations of heat storage (see Sections 4.1 and 9.1).
- Convective fluxes of latent (LE) and sensible (H) heat were measured directly via the eddy covariance technique.
- Net CO_2 flux (Fe_{CO2}) was measured using an eddy covariance system; this system consisted of a single-axis sonic anemometer and a fast-response infrared CO_2 gas analyzer. The air intake was located at the same level as the sonic anemometer, and air was drawn down to the gas analyzer at the base of the tower. Lag times between the gas analyzer signal and the sonic anemometer signal were included in the online processing of the flux; offline processing included heat flux density corrections (Webb et al., 1980) and CO_2 storage in the air layer between the intake and the surface.

Flux data were supported with accompanying meteorological measurements. At each site, profiles of wind speed, temperature, and humidity were measured in the lower boundary layer. In addition, soil and biomass temperatures, wind direction, and rainfall were monitored.

Tower data at both sites were collected from 15-Aug to 31-Aug-1993. In 1994, the YJP tower was operational almost continuously from 23-May to 30-Sep, and the fen tower was operational from 08-Apr to 23-Sep. Before 01-Jun, only convective energy fluxes and the supporting profile data were measured at the fen to support an associated hydrological study of snowmelt in an adjoining basin during the Focused Field Campaign (FFC) from 12-Apr to 02-May. CO_2 flux data came online at the fen by 01-Jun-1994. In 1995, only the fen was operational to support the continuation of the hydrological experiment; data were collected from the tower from 15-Apr to 10-Jun. In 1996, the measurement period at the YJP extended from 08-May to 07-Nov; at the fen data were collected from 29-Apr to 05-Nov.

Biophysical Measurements
The micrometeorological data at YJP were supplemented with biophysical data collected from areas surrounding the tower. These measurements included (h), (dbh), (LAI), and stomatal conductance of the coniferous overstory. The measurements, combined with the tower data, represent the basis for intersite comparisons of surface-atmosphere interactions.

1.6 Related Data Sets
BOREAS AFM-07 SRC Surface Meteorological Data
BOREAS HYD-01 Volumetric Soil Moisture Data
BOREAS TF-10 NSA-Fen Tower Flux and Meteorological Data
BOREAS TF-04 SSA-YJP Tower Flux and Meteorological Data

2. Investigator(s)

2.1 Investigator(s) Name and Title

Dr. J. Harry McCaughey (Principal Investigator (PI) at YJP)
Department of Geography
Queen's University

Dr. Dennis E. Jelinski (PI at Fen)
Department of Geography
Queen's University

Two PIs were associated with the Tower Flux (TF)-10 group: Harry McCaughey and Dennis Jelinski. Harry McCaughey oversaw the tower fluxes at both the YJP and the fen, and Dennis Jelinski was responsible for the vegetation work at the fen. Peter Lafleur shared responsibility for measurements at both sites. In addition, a large group of very competent graduate students, field assistants, and technicians contributed to the overall success of the work. Special mention goes to David Joiner and Paul Bartlett (Queen's University). David developed and built the CO_2 measurement system. Paul started work as a technician in the group and later stayed at Queen's as a doctoral student. He made many contributions, but special mention must go to his work on assembling and organizing the deployment of equipment in 1993 and to his porometry work at the YJP site in 1994 and 1996. Andrew Costello, Queen's, helped in the field setup in 1993 and did most of the initial stand measurements on the YJP canopy. He was assisted by Blair Mantha from Trent. Bob Metcalfe, Queen's and Trent, worked on an associated hydrology project focused upon the feeder basin north of the fen. He was supervised jointly by Jim Buttle, Trent University, and Harry McCaughey. Mike Skarupa and Greg Bryant, Trent, assisted in the data collection efforts at both sites. Kristan Boudreau was an outstanding field assistant, and she performed excellent work in 1994 in all facets of the experiments at both sites. Bruce Robertson and Derek Mueller were able field assistants in 1996. Finally, a special thanks to Laura Liblik, who did the majority of the work associated with the preparation of the data set before its submission to the BOREAS Information System (BORIS). Her attention to detail, her writing, and her editorial skills are much appreciated.

2.2 Title of Investigation

Surface Energy and Water Balances of Forest and Wetland Subsystems in the Boreal Forest - Surface Atmosphere Links and Ecological Controls

2.3 Contact Information

Contact 1:
Dr. J. Harry McCaughey
Dept. of Geography
Queen's University
Kingston, ON
CANADA
K7L 3N6
(613) 545-6035
(613) 545-6122 (fax)
mccaughe@post.queensu.ca

Contact 2:
Dr. Peter M. Lafleur
Dept. of Geography
Trent University
Peterborough, ON
CANADA
K9J 7B8
(705) 748-1487
(705) 748-1205 (fax)
plafleur@trentu.ca

Contact 3:
Dr. Dennis Jelinski
School of Environmental Studies
Queen's University
Kingston, Ontario
CANADA
K7L 3N6
(613) 545-6875
(613) 545-6617 (fax)
dj4@qsilver.queensu.ca

Contact 4:
K. Fred Huemmrich
University of Maryland
Code 923
NASA GSFC
Greenbelt, MD 20771
(301) 286-4862
(301) 286-0239 (fax)
Karl.Huemmrich@gsfc.nasa.gov

3. Theory of Measurements

Many of the individual measurements made during the study involved routinely collected data obtained with a single instrument (e.g., incoming solar radiation and temperature measurement with thermocouples). Such measurements represent standard data collection techniques, and specific, detailed elaboration is not provided in this report. However, there is discussion of some limited aspects of these routine measurements where such detail is required for a complete understanding. Readers are referred to the manufacturers' specifications for details on the theory of measurement and operation of individual instruments.

The following section describes only the measurement method used for the fluxes.

Sensible (H) and latent (LE) heat fluxes and the net flux of CO_2 (Fe_{CO2}) (net ecosystem exchange, NEE) were found using the eddy covariance technique (Campbell and Unsworth, 1979; Tanner et al., 1993). Fluxes are computed as the time-averaged product of the fluctuations of vertical wind velocity (w') and fluctuations of the appropriate scalar (the covariance). For example, fluctuations of temperatures (T') for H, water vapor density (q') for LE, and CO_2 concentration (C') for Fe_{CO2}, give:

$$LE = L <w'q'> \qquad (3.1)$$

$$H = rho\ Cp <w'T' \qquad (3.2)$$

$$FeCO_2 = rho(c) <w'C' \qquad (3.3)$$

where L is the latent heat of vaporization of water (J/kg), rho is the density of air (kg/m^3), Cp is the specific heat of air at constant pressure (J/kg/°C), rho(c) is the density of CO_2 (kg/m^3), and the < > symbol represents a time-averaged product or covariance.

In practical terms, the eddy covariance technique is very sensitive to site conditions and instrument response. For one-dimensional measurements, the site is assumed to be perfectly flat. This eliminates net positive or negative horizontal advection. Ideally, the response time of the instrument should be fast enough to monitor the complete spectrum of frequencies occurring in the turbulent flow. However, the total response is determined by the response time of the individual sensor, the instrument size and orientation, and the capacity to monitor the signal. Where two sensors are required, one to monitor w' and the other to monitor the appropriate scalar variable (T', q', or C'), then separation of the instruments in horizontal space introduces a possible error of mismatched frequencies sensed by the two systems. It is desirable to have the instruments as close together as possible; however, this can result in distortion of the wind field of one instrument by the presence of the other. A compromise is needed to overcome these two opposing problems, and sensors are typically placed 0.30 m to 0.40 m apart. Given the current status of data logging capacity, eddy covariance instruments are usually sampled at a rate of 10 Hz or greater.

4. Equipment

4.1 Sensor/Instrument Description

Micrometeorological Instruments
Meteorological and flux data at both sites were collected with similar instrumentation. Instruments were mounted on towers as described in Section 4.1.2. A listing of instrumentation follows.
- Net radiation was measured with a net pyrradiometer (model CN-1 Middleton, Carter-Scott Design, Victoria, Australia) aspirated with dry nitrogen gas.
- Incoming and outgoing solar radiation were measured with pyranometers (model 8-48, Eppley Laboratories, Inc., Newport, RI, USA).
- Outgoing longwave radiation was measured with a pyrgeometer (model PIR, Eppley Laboratories, Inc., Newport, RI, USA).
- Incoming and outgoing PPFD were measured with quantum sensors (model LI-Q190SA, LI-COR, Inc., Lincoln, NE, USA).
- Absolute wet- and dry-bulb temperatures were measured with psychrometers constructed from PVC tubing covered with reflective tape. Ventilation was supplied by a 12-volt DC fan that gave an air flow between 4-6 m/s across the sensor. The sensors were single-junction 24 a.w.g. copper-constantan thermocouples sealed with epoxy in stainless steel tubing (250 mm in length, 3.5 mm in diameter). The wet-bulbs were covered with cotton wicking to a length of 150 mm.
- Wind speeds were measured with 3-cup anemometers (model 12102, R.M. Young Co., Traverse City, MI, USA). The anemometers contain a DC generator that produces an analog signal proportional to wind speed.
- Wind direction was measured with a vane (model 12302, R.M. Young Co., Traverse City, MI, USA) containing a potentiometer that designates direction as proportional to the voltage output.
- Rainfall was measured with tipping bucket gauges (YJP: model P501, Weathermeasure Corporation, Sacramento, CA, USA; Fen: model TE252M, Campbell Scientific, Inc., Logan, UT, USA).
- Soil temperatures were measured with single-junction copper-constantan thermocouples (24 a.w.g.) fixed into a 3.18-cm-diameter wooden dowel inserted into the soil. Two soil temperature rods were installed at each site in order to sample soil temperatures below different cover types.

At YJP, one rod was placed 14 m from the tower at 323° among young jack pine trees 1.5 m in height. In 1993, temperatures only from 1-, 5-, and 10-cm depths are available from the north site. Temperatures from 1-, 5-, 10-, 25-, 50-, and 75-cm depths are available from this site in 1994. The second rod was placed 6.7 m to the west of the tower (253°) among trees 2-3 m in height. Temperatures at the west site were recorded at depths of 1, 5, 10, 25, 50, 75, and 100 cm in both years.

- Soil heat flux was measured at each site with two soil heat flux plates (model HFT-3, Radiation Energy Balance Systems, Inc. (REBS), Seattle, WA, USA). Values from these instruments, combined with the soil temperature profiles, were used to calculate soil heat flux at each site as follows. At YJP, measurements were obtained at a depth of 10 cm below the soil surface. Heat storage in the soil layer above the heat flux plates was calculated using temperatures measured at the 1-cm, 5-cm and 10-cm levels (see Section 9.1).

- All tower variables (except eddy covariance) were recorded on data loggers (model CR7X, Campbell Scientific, Inc., Logan, UT, USA). The eddy covariance signals were recorded on data loggers (model 21X, Campbell Scientific, Inc., Logan, UT, USA).

- CO_2 concentration and flux densities were measured with a system designed at Queen's University by D. Joiner. It consisted of a single-axis sonic anemometer (mentioned above) and a fast response infrared gas analyzer (IRGA) (model LI-6252, LI-COR, Inc., Lincoln, NE, USA).

    Air is drawn by an AC pump from the intake of a tube (1/4" i.d. Bev-a-line IV) situated on the sonic anemometer arm to the IRGA at the base of the tower. The flow is split before reaching the IRGA, and the line to the IRGA passes through a fine particle filter. Air from the IRGA passes a pressure transducer (model PX142, Omega Engineering, Stamford, CT, USA) and a mass flow sensor (model 5860E, Brooks Instruments Division, Hatfield, PA, USA).

    Cross-correlation analysis was used to determine the travel time of the air from the tube inlet to the gas analyzer. The flux density of carbon dioxide was then determined with the eddy covariance technique by finding the covariance of the 10-Hz direct output from the gas analyzer with time-lagged vertical wind velocity measured with a one-dimensional sonic anemometer (model CA-27, Campbell Scientific, Inc., Logan, UT, USA).

    The direct output from the IRGA was calibrated once a day using calibration gases flowing through the gas analyzer at the same pressure as that of the air down the tower. These field calibrations, linear over the range of ambient carbon dioxide concentrations and unchanging with temperature, were constantly corrected for pressure changes recorded with the gauge pressure transducer.

    Data processing and storage were done on data loggers (model 21X, Campbell Scientific, Inc., Logan, UT, USA), using the covariance at 10 Hz data and a 15-minute averaging subinterval. The CO_2 flux data were corrected for fluctuations of temperature and water vapor density during postseasonal analysis (Webb et al., 1980).

    Absolute concentrations of CO_2 were calculated using the factory calibration equation supplied with the LI-6252 and were corrected for air pressure fluctuations. Station values for air pressure were obtained from the Thompson airport and entered daily as a constant into the data loggers. Daily field calibration of the IRGA showed that the absolute concentration may exhibit a drift of up to 3 ppmv over a 24-hour period.

    Final CO_2 flux density values combine the contributions from both the eddy flux and the changes in CO_2 storage for the volume of air beneath the eddy covariance instruments.

Biophysical Instruments

- Biomass temperatures at YJP were measured with copper-constantan parallel thermocouples (30 a.w.g.) embedded directly into the boles. Thermojunctions were placed at the approximate center of the biomass volume (1/3 of the way up the tree and 1/3 of the radius into the boles) (McCaughey and Saxton, 1988; Saxton and McCaughey, 1988). Four parallel thermocouples, each one consisting of three thermojunctions wired in parallel, were used. One set was placed in three large trees (~5.0 m in height) 12.6 m from the tower at 185°, the second set was placed in three medium trees (~2.5 m in height) 9.6 m from the tower at 218°, the third set was placed in three small trees (~1.5 m in height) 14 m from the tower at 230°, and the fourth set was placed in three small trees (~1.5 m in height) near the northern soil heat flux plate at 323°.
- Leaf stomatal conductance was measured with a steady state diffusion porometer (model LI-1600, LI-COR, Inc., Lincoln, NE, USA). Measurements on jack pine shoots required that the sensing head was fitted with a cylindrical chamber (model LI-1600-07, LI-COR, Inc., Lincoln, NE, USA).
- Projected LAI was measured with an optical Plant Canopy Analyzer (model LAI-2000, LI-COR, Inc., Lincoln, NE, USA).

4.1.1 Collection Environment

The instruments were operated mainly under summer conditions with maximum temperatures around 35 °C. Data were collected over the growing season of 1994 and the spring through fall/winter of 1996. In the spring and fall/winter seasons, more extreme low temperatures were experienced. During these periods, the environment was more severe, and freezing temperatures were common; the lowest temperatures experienced were around -30 °C.

4.1.2 Source/Platform

The towers erected at YJP and fen were 12-meter-tall triangular communications type, guyed on three sides, and anchored into the mineral soil. At both sites, all sensors were mounted on the towers with fixed aluminum (3.18 cm diameter) extension arms, with the exception of the eddy covariance equipment, which was mounted on a swivel system allowing for orientation of the instruments into the wind. Sensor height above the surface, distance from the tower, and orientation (degrees from magnetic north) are given for the YJP in Table 1.

Biomass temperatures were measured at two sites in the vicinity of the flux tower at YJP. One site, directly west of the tower, was named the "west site," and the other, located north of the tower, was named the "north site." Biomass temperature sensors consisted of three-junction parallel thermocouples, and one thermojunction was inserted into three separate trees in three chosen height categories (small, medium, and large) at the west site. At the north site, only small trees existed. Each thermojunction was inserted into the bole to a depth of one-third the radius depth at a height of one-third the height of the tree (see Section 4.1). Table 2 shows the height and dbh for all trees sampled at the two measurement sites.

Table 1. Sensor heights on the flux tower at the YJP in 1993, 1994, and 1996. The orientation of the arm holding the sensor is given in degrees measured from magnetic north, and the distance (m) from the tower is given. The symbol n/a, indicating "not applicable," means that no measurements were taken. The orientation of the arm holding the sonic anemometer and the krypton hygrometer was variable on a swivel mount that could be set anywhere from 120° from magnetic north through 360° to 25° from magnetic north.

Table 1. Sensor heights on the flux tower at the YJP in 1993, 1994, and 1996.

Variable [Sensor]	Height (m)			Distance (m)	Orientation (degrees)
	1993	**1994**	**1996**		
Incoming Solar Radiation [pyranometer]	11.82	11.82	11.82	1.5	143
Outgoing Solar Radiation [pyranometer]	11.58	11.58	11.58	1.5	143
Outgoing Longwave Radiation [pyranometer]	11.38	11.38	11.38	1.5	203
Net Radiation [net pyrradiometer]	11.70	11.70	11.70	2.3	133
Incoming PPFD [quantum sensor]	11.54	11.54	11.54	1.5	213
Outgoing PPFD [quantum sensor]	11.36	11.36	11.36	1.5	213
Wet- and Dry-bulb Temperatures [thermocouples]					
Canopy	1.60	1.60	n/a	1.5	233
Level 1	5.10	5.17	5.17	0.8	233
Level 2	6.10	6.10	n/a	0.8	233
Level 3	7.10	7.15	n/a	0.8	233
Level 4	9.10	7.70	7.70	0.8	233
Level 5	11.10	10.30	10.30	0.8	233
Wind Direction [vane]	11.10	10.30	10.30	1.8	323
Wind Speed [cup anemometer]					
Level 1	5.10	5.17	5.17	1.5	323
Level 2	6.10	6.10	n/a	1.5	323
Level 3	7.10	7.15	n/a	1.5	323
Level 4	9.10	7.70	7.70	1.5	323
Level 5	11.10	10.30	10.30	1.5	323
Vertical Wind Speed [sonic anemometer]	9.35	9.00	9.00	1.0	120-360-25
Vapor Density [krypton hygrometer]	9.35	9.00	9.00	1.0	120-360-25
Relative Humidity [T/RH sensor]	n/a	n/a	10.30	0.2	232

Table 2. Location of biomass temperature sensors at the west and north measurement sites at YJP. The same locations were used in all three experimental years: 1993, 1994, and 1996. h is tree height (m) and dbh (m) is the diameter at breast height. At the west site, three sizes of trees were sampled: small, medium, and large. Three trees in each size range were sampled with three-junction parallel thermocouples, and one thermojunction was located in each tree.

Table 2. Location of biomass temperature sensors at the west and north measurement sites at YJP.

	h(m)	dbh(m)
West site:		
small trees	1.45	0.0045
	1.20	<0.0030
	1.75	0.0070
medium trees	2.70	0.0210
	2.35	0.0160
	2.90	0.0190
large trees	5.80	0.0600
	4.20	0.0420
	4.30	0.0430
North site:		
small trees	1.75	0.0120
	1.72	0.0088
	0.97	<0.0030

4.1.3 Source/Platform Mission Objectives

The primary objective of the team was to collect and analyze the micrometeorological data from the two flux towers on a continuous basis during all of the experiments. In addition, data were assembled to characterize the surface's state in terms of LAI, type, distribution, height, and density of the vegetation, and stomatal conductance at the YJP only. Subsidiary experiments in 1996 at the YJP measured soil evaporation, throughfall, and rainfall interception of the canopy.

4.1.4 Key Variables

The key meteorological variables are incoming and reflected solar radiation, PPFD, outgoing terrestrial radiation, net radiation, wet- and dry-bulb temperatures, wind speed, wind direction, latent and sensible heat fluxes, net CO_2 flux, soil temperature, biomass temperature, rainfall, and water level. The key biophysical variables are LAI, leaf stomatal conductance, h, stem density, and dbh.

4.1.5 Principles of Operation

Sonic Anemometer

The sonic anemometer system (model CA27, Campbell Scientific ,Inc., Logan, UT, USA) obtains the velocity fluctuations of vertical wind speed from the measured Doppler shift induced by the wind velocity on an ultrasonic frequency pulse broadcast across a 10-cm path. The effect of temperature on sound velocity is eliminated by determining the Doppler frequency from the difference between forward and reverse path observations. Electronic processing of the signals from the ultrasonic transducers produces a real-time analog output voltage in the range ±4.0 V DC.

Air temperature fluctuations for the Campbell Scientific eddy covariance system are measured with a fine-wire thermocouple mounted about 4 cm from the anemometer sound path. The thermocouple output is amplified to a ±4.0 V DC signal. The thermocouple temperature is referenced to the instrument case, which is thermally lagged and responds slowly to temperature changes.

Absorption Hygrometer

The absorption hygrometer (model KH20, Campbell Scientific, Inc., Logan, UT, USA) measures the ultraviolet light transmission across a nominal 1-cm path in a water vapor absorption band corresponding to a krypton emission line (Campbell and Tanner, 1985). Instrument response is at least sufficient to resolve fluctuations of 80 Hz. The instrument output is a voltage in the range 0 to 4 V DC. The signal strength may be subject to gradual diminution as a result of scale accumulation on the optical surfaces.

Longwave Radiation Measurement

The sensing surface of a pyrgeometer (model PIR, Eppley Laboratories, Inc., Newport, RI, USA) consists of a differential thermopile that measures net longwave radiation fluxes between itself and the sky or ground (depending on orientation). The dome of the pyrgeometer is composed of silicon with a vacuum-deposited interference filter on its inner surface. The composite dome transmission shows an abrupt transition between approximately 3 and 4 micrometers from complete opaqueness to maximum transparency.

The outgoing longwave radiation from the instrument is calculated using the temperature of its blackbody cavity and the Stefan-Boltzmann equation. This flux is added to the thermopile signal to get the total incoming flux. The temperature of the blackbody radiator can be measured using a thermistor.

The thermopile output signal is measured as a single-ended voltage in the Campbell Scientific CR7X data logger. The case thermistor is not polarized, and is connected between an analog input channel and ground. A 1000-ohm resistor is connected between the analog input channel and a switched analog output channel (725 card). The thermistor is excited with 1350 mV across the 1000-ohm resistor, and the thermistor (pyrgeometer) temperature is calculated as a function of the thermistor voltage (a function of its resistance). This method corresponds to the protocol for using the Eppley pyrgeometer proposed by the National Atmospheric Radiation Center (NARC). This method does not use the pyrgeometer's battery-powered temperature compensation circuit, and no battery should be installed when using the pyrgeometer in this manner.

Plant Canopy Analyzer

The plant canopy analyzer (model LAI-2000, LI-COR, Inc., Lincoln, NE, USA) is composed of a LAI-2070 control unit and a LAI-2050 sensor head. The sensor head projects the image of its nearly hemispheric view onto five detectors arranged in concentric rings (approximately 0-13, 16-28, 32-43, 47-58, and 61-74 degrees of zenith angle). Radiation above 490 nm is rejected. Data are stored and processed in the control unit. LAI is calculated by the reduction in light intensity measured between an above-canopy reading and a below-canopy reading. Normally, simultaneous measurements of these two quantities can be achieved with two sensors connected to the same control unit. Where this is not possible, two sensors and separate control units can be used and the data later integrated, or a single sensor and control unit is used for above- and below-canopy measurements. The LAI value obtained from the LAI-2000 relates directly to projected leaf area; corrections can be applied for clumping within the canopy or conversion to total surface area. For further information, consult the LAI-2000 plant canopy analyzer instruction manual.

Diffusion Porometer

Leaf stomatal conductance was measured with a steady state porometer (model LI-1600, LI-COR, Inc., Lincoln, NE, USA). Leaf samples are placed in contact with a cuvette by clamping a portion of the leaf over an aperture in the cuvette wall. The relative humidity in the cuvette is held constant by flowing dry air directly into the cuvette at an appropriate rate.

Diffusive resistance/conductance is determined by measuring the flow required to obtain a balance between the flux of water transpired from the leaf and the flow of moist air out of the cuvette at a set humidity (usually ambient). The instrument also measures leaf temperature, cuvette temperature, and transpiration rate. For measurements of coniferous needles, the LI-1600-07 cylindrical chamber is used. This allows a small portion of a branch containing needles to be inserted into the cuvette. The LI-1600 is also outfitted with a quantum sensor for instantaneous measurement of PPFD.

4.1.6 Sensor/Instrument Measurement Geometry
See Table 2 in Section 4.1.2.

4.1.7 Manufacturer of Sensor/Instrument
Mass flow sensor and control unit for eddy covariance system:
Brooks Instruments Division
Emmerson Electric Co.
407 W. Vine St.
Hatfield, PA 19440
USA
(215) 362-3500

Sonic anemometer; krypton hygrometer; fine-wire thermocouple; CR7X and 21X data loggers; rain gauge (fen):
Campbell Scientific, Inc.
P.O. Box 551
Logan, UT 84321
USA
(519) 354-7356

Pyranometer; pyrgeometer:
Eppley Laboratories, Inc.
P.O. Box 419
Newport, RI 02840
USA
(401) 847-1020

LAI-2000 Plant canopy analyzer; diffusion porometer; quantum sensor; CO2 IRGA:
LI-COR, Inc.
4421 Superior Street
P.O. Box 4425
Lincoln, NE 68504
USA
(402) 467-3576

Net pyrradiometer:
Carter-Scott Design
22 Ailsa Street
Box Hill
Victoria, 3128
AUSTRALIA
+61-3-9899-4277

Pressure transducer; thermocouple wire:
Omega Engineering
One Omega Drive
P.O. Box 4047
Stamford, CT 06907
USA
(203) 359-1660

Soil heat flux plate:
REBS
P.O. Box 15512
Seattle, WA 98115-0512
USA
(206) 624-7221
Cup anemometer; wind vane:
R.M. Young Co.
2801 Aero Park Drive
Traverse City, MI 49648
USA
(616) 946-3980

Rain gauge (YJP):
Weathermeasure Corporation
P.O. Box 41257
Sacramento, CA 95841
USA
(916) 481-7565

4.2 Calibration

Pyranometers, pyrgeometers, and net pyrradiometers used at both sites were calibrated at NARC, Atmospheric Environment Service (AES), Downsview, Ontario. Following the intersite calibration on net pyrradiometers performed in the field in 1994 with the roving REBS 6-net pyrradiometer (Hodges and Smith, 1997; Smith et al., 1997), a corrected set of net radiation data was calculated for the 1994, 1995, and 1996 experimental periods for both the fen and YJP. The corrected net radiation data will potentially facilitate the intercomparison of flux behavior between the tower flux sites.

CO_2 concentrations for high- and low-span calibration gases were determined at the Carbon Cycle Research Section, AES, Downsview, Ontario, Canada.

Factory calibrations were used for several instruments, and the recalibration details for individual sensors are given below.

The details of the recalibration performed on the porometers (LI-COR, Inc., Lincoln, NE, USA) used in the experiments are given in Section 4.2.2.

Following the 1993 field experiment, each individual calibration for the group of cup anemometers and wind vane (R.M. Young Co., Traverse City, MI, USA) was checked using the wind tunnel at Trent University, and no changes were needed to the original factory calibrations. Because the potentiometers on the two wind vanes were set in the field each time the instruments were deployed, both can be considered to have had regular field calibration checks.

For the soil heat flux plates (REBS, Seattle, WA, USA), the factory calibrations were accepted for all four transducers, two at each site.

Routine calibration checks were done on all rain gauges (Campbell Scientific, Inc., Logan, UT, USA, and Weathermeasure Corporation, Sacramento, CA, USA) by pouring a known amount of water into the gauge and noting the response. In all cases, the gauges were within the manufacturer's specification.

The sonic anemometers and krypton hygrometers (Campbell Scientific, Inc., Logan, UT, USA) at both the fen and YJP sites were recalibrated in March 1994 following the 1993 experiment and before

redeployment for the 1994 experiment. Minor changes resulted, but they were not large enough to require correction to the 1993 data.

For all thermocouples, the appropriate calibration equation available in the data loggers (Campbell Scientific, Inc., Logan, UT, USA) was used.

4.2.1 Specifications

Whenever a new calibration was determined for an instrument, the new calibration was applied from the time of the recalibration. There was no attempt to blend the calibrations before and after the recalibration. Any step-up or step-down in the data values as a result of recalibration was accepted. For all instruments, the calibration changes were minor, and there were no instances where a blending of the calibrations was necessary.

4.2.1.1 Tolerance

The precision of the measured meteorological variables and the corresponding transducers are summarized below. In the following list, micromole is abbreviated to μmol.

Variable	Transducer	Precision
solar radiation	Eppley pyranometer	1 W/m^2
longwave radiation	Eppley pyrgeometer	1 W/m^2
net radiation	Middleton net pyrradiometer	1 W/m^2
PPFD	LI-COR quantum sensor	1 μmol/m^2/s
carbon dioxide concentration	LI-COR IRGA	1 ppmv
soil heat flux	REBS heat flux plate	1 W/m^2
air, soil, and biomass temperature	Copper/constantan thermocouple	0.1 °C
horizontal wind speed	R.M. Young cup anemometer	0.1 m/s
wind direction	R.M. Young wind vane	1°
relative humidity	R.M. Young T/RH sensor	1%
vertical wind speed	Campbell Scientific sonic anemometer	0.1 m/s
rainfall	Campbell Scientific tipping bucket	0.1 mm
rainfall	Weathermeasure tipping bucket	0.254 mm

4.2.2 Frequency of Calibration

All radiometers used in the study were on a regular, 2-year calibration cycle. This calibration frequency was increased during BOREAS, and each radiometer was calibrated before each major field experiment. Full calibrations were done in April 1994, October 1994, and March 1996.

One sonic anemometer (model CA27, Campbell Scientific, Inc., Logan, UT, USA) was recalibrated by the manufacturer in May 1995 following water damage to the instrument in September 1994 at the fen.

Two porometers (model 1600, LI-COR, Inc., Lincoln, NE, USA) were used in the study. Each one was calibrated by the manufacturer prior to the 1993 field experiment; they were also intercalibrated. The single one that continued to be used in 1996 at the YJP was recalibrated by the manufacturer in April 1995.

The krypton hygrometers from the YJP and fen were calibrated in 1993 before deployment in the field and were recalibrated in March 1994.

Calibrations were determined on all CO_2 reference gas tanks prior to both major field seasons in March 1994 and March 1996.

Routine calibration checks were made on the rain gauges, following the protocol suggested by the manufacturers, prior to their deployment in all field experiments. No calibration change was necessary to either gauge.

4.2.3 Other Calibration Information

A summary follows of the instruments used at each site along with their calibration histories.

Solar radiation was measured using Eppley pyranometers. The instruments, identified by serial number, used at both sites for each experiment are given in Table 3.

Table 3. Eppley pyranometers used at the YJP and Fen in all experimental years. Each pyranometer is identified by its serial number.

Table 3. Eppley pyranometers used at the YJP

Variable	Year			
	1993	**1994**	**1995**	**1996**
Kd	13762	15889	------	15889
Ku	13855	14713	------	14713

The calibration histories of the pyranometers are shown in Table 4. All calibrations remained stable through the BOREAS field periods, and the largest change in any calibration was -0.57%.

Table 4. Calibration history of the Eppley pyranometers used in all experimental years. The change in calibration is given as a percentage from the previous value. The units of calibration are microvolts/W/m^2.

Table 4. Calibration history of the Eppley pyranometers

Serial number	Year	Calibration	%change in calibration
13762	1992	12.21	-1.12
	1994	12.14	-0.57
	1996	12.20	0.49
13855	1992	10.92	-0.55
	1994	10.89	-0.27
	1996	10.92	0.28

14713	1992	11.17	-0.62
	1994	11.14	-0.27
	1996	11.14	0.00
15889	1992	11.09	-1.10
	1994	11.05	-0.36
	1996	11.06	0.09

Longwave radiation was measured using Eppley pyrgeometers. Instrument 20837F3 was used at YJP in 1993, 1994, and 1996, and instrument 29583F3 was used at Fen from 1993 to 1996. The calibration history of each instrument is given in Table 5. The first calibration of instrument 29583F3 in 1994 proved to be wrong because of a malfunctioning reference temperature bath NARC. This was corrected by a recalibration of the instrument the same year, and all of the data were corrected in postprocessing.

Table 5. Calibration history of the Eppley pyrgeometers used in all experimental years. The change in calibration is given as a percentage from the previous value. The units of calibration are microvolts/W/m^2.

Table 5. Calibration history of the Eppley pyrgeometers

Serial number	Year	Calibration	% change in calibration
20837F3	1992	3.96	-2.22
	1994	3.88	-2.02
	1996	3.86	-
29583F3	1993	3.97	-
	1994	3.62	-8.82 (calibration is suspect)
	1994	3.83	-3.53 (recalibration for 1994)
	1996	3.83	0.00

Net radiation was measured using Middleton net pyrradiometers. The instruments used are listed in Table 6.

Table 6. Middleton net pyrradiometers used in the field experiments. Each instrument is identified by serial number.

Table 6. Middleton net pyrradiometers

Serial number	Site
1330	Fen in 1993, and from DOY 97-145 in 1996
1333	Fen in 1994, and 1995, and from DOY 146 in 1996
1408	YJP in 1993, 1994, and 1996

The calibration histories of the net pyrradiometers are given in Table 7. For all net pyrradiometers, the calibration values are given separately for shortwave (SW), longwave (LW), and combined - the arithmetic average of SW and LW. The combined value was used for all times of the day, including the nighttime, when only longwave radiation is present. All instruments had two calibrations in 1994. The first calibration proved to be wrong because of a malfunctioning reference temperature bath at NARC. This was corrected by a recalibration of the instrument the same year, and all of the data were corrected in postprocessing. With the exception of the aberrant first calibration in 1994, all instruments remained stable for the duration of the experiments; the largest change was less than 4% and was normally less than 1%.

Table 7. Calibration history of the Middleton net pyrradiometers used in all experimental years. The change in calibration is given as a percentage from the previous value. The units of calibration are microvolts/W/m^2. Separate calibrations are given for shortwave (SW), longwave (LW), and combined - the arithmetic average of the SW and LW values. The calibration constant (cal. constant) is the ratio of the SW to LW calibration.

Table 7. Calibration history of the Middleton net pyrradiometers

Serial number	Year	SW	% change SW	LW	% change LW	combined	% change combined	cal. constant
1330	1992	37.52	-0.87	35.18	-3.98	36.35	-2.42	1.07
	1994	38.16	1.17	32.40	-7.90	35.28	-2.94	1.18
	1994	37.55	0.08	34.82	-1.02	36.19	-0.44	1.08
	1996	35.54	-5.35	34.13	-1.98	34.84	-3.73	1.04
1333	1992	37.74	-2.15	34.90	-6.46	36.32	-4.27	1.08
	1994	38.41	1.78	32.85	-5.87	35.63	-1.90	1.17
	1994	38.17	1.14	34.62	-0.80	36.39	0.22	1.10
	1996	38.12	-0.13	35.17	1.59	36.64	0.69	1.08
1408	1992	38.58	-1.36	35.99	-5.01	37.28	-3.14	1.07
	1994	38.53	-0.13	35.83	-0.44	37.18	-0.29	1.08
	1996	38.17	-0.93	35.36	-1.30	36.77	-1.10	1.08

PPFD was measured using LI-COR, Inc., quantum sensors. Table 8 shows the instruments used at each site in each experimental year, and Table 9 gives the calibration constants.

Table 8. Quantum sensors used at the experimental sites and the variables measured: PPFDd is incoming PPFD, and PPFDu is reflected PPFD. Instruments are identified by serial number.

Table 8. Quantum sensors used

Serial number	Site	Variable
Q17605	Fen 1993 to 1996	PPFDd
Q16754	Fen 1993 to 1996	PPFDu
Q17614	YJP 1993, 1994, 1996	PPFDd
Q17613	YJP 1993, 1994, 1996	PPFDu

Table 9. Calibration constants in units of $\mu mole/s/m^2/mv$ for the quantum sensors used in the experiments. The instruments are identified by serial number.

Table 9. Calibration constants

Serial	Calibration
Q17613	295.12
Q17614	307.74
Q17605	293.25
Q16754	355.87

CO_2 concentration and CO_2 flux density were measured using an IRGA (model LI-6252, LI-COR, Inc., Lincoln, NE, USA) and a sonic anemometer (model CA27, Campbell Scientific, Inc., Logan, UT, USA). Table 10 lists the IRGAs and the sonic anemometers used at both sites. Sonic 1353 was damaged by water seeping into the lower arm at the conclusion of the 1994 experiment. This instrument was repaired and recalibrated before being deployed again in 1996.

Table 10. The sonic anemometers and IRGAs used at the fen and YJP. The instruments are identified by serial number. There was no CO_2 flux measured at the fen in 1995; the sonic measured the convective fluxes only.

Table 10. The sonic anemometers and IRGAs

	Serial number	Site
Sonic anemometer	1201	Fen in 1995, YJP in 1993, 1994, and 1996
	1353	Fen in 1993, 1994, and 1996
IRGA	IRG2-208	Fen in 1993, 1994, and 1996
	IRG2-209	YJP in 1993, 1994, and 1996

Soil heat flux was measured using REBS soil heat flux plates. The calibrations of the plates and the sites where they were deployed are given in Table 11.

Table 11. Calibrations for the soil heat flux plates, in units of $W/m^2/mV$, and the sites where they were deployed. Individual plates are identified by serial number.

Table 11. Calibrations for the soil heat flux plates

Serial number	Calibration	Site
933060	40.0	Fen in 1993, 1994, 1995, and 1996
933061	38.7	Fen in 1993, 1994, 1995, and 1996
933062	39.0	YJP in 1993, 1994, and 1996
933063	40.7	YJP in 1993, 1994, and 1996

Horizontal wind speed was measured using 3 cup anemometers (model 12102, R.M. Young Co., Traverse City, MI, USA). These instruments have calibrations in units of mv at 1800 rpm, and this is combined with a second general calibration equation to convert rpm to m/s. The calibrations of the anemometers are given in Table 12.

Table 12. Calibration of the 3-cup anemometers used at each site for horizontal wind speed measurement at the levels identified, e.g., U1 is the anemometer at level 1. The units of the calibration are mv at 1800 rpm.

Table 12. Calibration of the 3-cup anemometers

Site: YJP

Level	1993	1994	1995	1996
U1	2400	2400	-	2400
U2	2398	2398	-	-----
U3	2404	2404	-	-----
U4	2404	2404	-	2404
U5	2402	2402	-	2402

Site: Fen

Level	1993	1994	1995	1996
U1	2400	2400	2400	-----
U2	2397	2397	2397	2397
U3	2396	2396	2401	2395
U4	2401	2401	2401	-----
U5	2399	2399	2399	2401

Relative humidity was measured using a combination temperature/relative humidity probe (model 41372VC, R.M. Young Co., Traverse City, MI, USA) at each site in 1996 (Table 13). The temperature is measured with an RTD sensor, and the relative humidity is measured with a capacitance element. This probe was ventilated naturally and shielded by a 12-level plate shield. Each probe has the same calibration and specifications (Table 14).

Table 13. Temperature/relative humidity sensors used at the sites in 1996.

Model	Serial number	Site
41372VC	1762	Fen
41372VC	1763	YJP

Table 14. Calibration and specifications for the temperature/relative humidity sensor (model 41372VC, R.M. Young Co., Traverse City, MI, USA).

Relative humidity:	operating temperature: -10 °C to 60 °C
	measuring range: 0 to 100%
	accuracy at 20 °C: 2% from 0-90% RH
	3% from 90-100% RH
	stability: better than ± 2% RH for 2 years
	response time: 15 sec
	sensor element: Vaisala intercap
	output signal: 0-1 volt DC
Temperature:	calibrated measuring range: -50 °C to 50 °C
	accuracy at 20 °C: ± 0.3 °C
	output signal: 0-1 volt DC

Rainfall was measured using tipping bucket rain gauges at both sites in all years. At the YJP, the gauge (model P510, Weathermeasure Corporation, Sacramento, CA, USA) was mounted at canopy top, and at the fen, the gauge (model TE525, Texas Instruments, supplied by Campbell Scientific, Inc., Logan, UT, USA) was at a height of 1 meter above the surface. For the Weathermeasure gauge, 1 tip equals 0.01 inches (0.254 mm of rain), and for the Texas Instruments gauge, 1 tip equals 1 mm of rain.

Leaf stomatal conductance was measured using a steady-state diffusion porometer (model LI-1600, serial number SSP1094, LI-COR, Inc., Lincoln, NE, USA). The onboard quantum sensor (serial number Q11174) has a calibration constant of 5.21 microamps/(1000 μmoles/s/m^2). This calibration remained stable from 1993 to the end of the experiment in 1996; there was no change at the 1995 recalibration.

Atmospheric pressure was measured at each site in 1996 using a Vaisala pressure transmitter (model PTB 101B, Vaisala, Oy, Finland, and supplied by Campbell Scientific, Inc., Logan, UT, USA). Each instrument had been calibrated against a working standard in February 1996. The instrument at YJP was S/N R0940044, and that at the fen was S/N R0940004.

5. Data Acquisition Methods

The outputs from all instruments producing voltages were recorded on data loggers. Data from the loggers' memories were downloaded at regular intervals to either cassette tape or electronic storage module, and all data were transferred in the field to microcomputers and backed up on either floppy diskette or 1-GB Jaz drives (Iomega Corporation, Fenton, MO, USA).

   Specific details for each major system are given below.
- Tower data (except eddy covariance). All signals were recorded on data loggers (model CR7X, Campbell Scientific, Inc., Logan, UT, USA) at a scan rate of once per 10 seconds. Output was processed every 3, 15, and 30 minutes depending on the variable. Only 30-minute data are reported in the BORIS data base.
- Eddy covariance. All signals were recorded on data loggers (model 21X, Campbell Scientific, Inc., Logan, UT, USA) at a scan rate of once per 0.1 seconds. Intermediate processing was done every 15 minutes and output data were processed every 30 minutes.
- Leaf conductance. Porometric data from the LI-1600 were recorded on cassette tapes and later downloaded to microcomputers. The measurement frequency was variable. Data were collected on selected days under chosen weather conditions and only when the canopy was dry. Typically, measurements started early in the morning and continued every hour until evening.
- Forest canopy measurements. Canopy parameters (dbh, h, stem density) were recorded manually in field notebooks and later transposed to digital files.

6. Observations

6.1 Data Notes

Biophysical Measurements
   The micrometeorological data at YJP were supplemented with biophysical data collected from areas surrounding the tower. These measurements included h, dbh, LAI, and stomatal conductance of the coniferous overstory. The measurements, combined with the tower data, represent the basis for intersite comparisons of surface-atmosphere interactions. The sections below include descriptions of the major sampling programs.

Forest Stand Parameters
   Forest stand parameters were measured along transects within the zone designated as the wind aligned blob (WAB), the area of the site, centered on the experimental tower and of radius 500 m, within which the majority of the surface fluxes originate. There was no sampling in the zone from 60° to 120°. The parameters measured included h, dbh, and stem density. Five transects were sampled in both 1993 and 1994. In 1993, each transect radiated a distance of 500 m from the tower to the edge of the WAB at orientations of 10°, 130°, 190°, 250°, and 310°. In 1994, the transects started at a distance of 125 m from the tower and continued out to 500 m at bearings of 40°, 160°, 220°, 280°, and 340°, which are midday between the orientations of the earlier lines. Two sampling methods were employed. First, in 1993, tree density and height were measured in square, 25 m² plots every 100 m along each transect. A total of 20 plots were measured, and these data were designated as quadrat data. Tree height was measured with a survey stadia rod or tape, and dbh for trees with h greater than 1.3 m was measured with calipers. Using a subsample of 312 trees, a relationship was found between dbh and h. This relationship was then used to calculate tree heights for all trees sampled subsequently along the transects. The results of the quadrat survey indicated significant variation in stand parameters between transects and within a single transect. For example, stem density varied from 8,000 to 11,000 trees/ha within the 20 sample plots. To investigate smaller-scale spatial variation, a denser sampling was conducted by measuring dbh and stem density every 10 m along all transects using the Point Center Quarter Method (PCQM) (Mueller-Dombois and Ellenberg, 1974). Trees with h >1.3 m and trees with

h < 1.3 m were sampled separately. A summary of the 1993 PCQM transect data is shown in Table 15. Aggregating these data revealed that the greatest stem density occurred within 200 m of the tower at a value of 20,000 trees/ha, and a decrease out to the edge of the WAB where the value dropped to around 10,000 trees/ha. The variation in stem density was associated with three vegetation patterns: dense cover of short trees, sparse cover of tall trees, and a mixture of short and long trees. The average tree height on the site was 2.27 m. Destructive sampling of nine trees yielded a value for the total green biomass of the canopy of 2.24 kg/m^2 using the model developed by Alemdag (1983).

Table 15. Average canopy parameters for the YJP site developed from PCQM data from five transects sampled in 1993. Each transect ran from the tower to the edge of the WAB, and samples were taken every 10 m. The orientation of the transects is from magnetic north. Units of measurement are as follows: dbh in cm, height in m, and stem density in trees/ha. Source: Costello (1995).

Table 15. Average canopy parameters for the YJP site

	Transect Orientation (degrees)				
Variable	10	130	190	250	310
dbh	1.39	1.77	1.51	2.05	1.60
Tree height	2.08	2.35	2.17	2.55	2.23
Stem density	16800	14400	7000	13200	10000
Number of samples	200	88	168	196	200

Stomotal Conductance

Stomatal conductance was measured with a steady-state diffusion porometer (model LI-1600, LI-COR, Inc., Lincoln, NE, USA) fitted with a cylindrical chamber aperture. Shoot samples were prepared at least 24 hours prior to the first measurements. Preparation involved isolating a clump of needles that would fit completely into the porometer's sample chamber. To achieve this, some needles were removed from the twig on either side of the sample clump. The bare twig, thus exposed, allowed the soft foam of the sample chamber to close around it and provided an air-tight seal around the sample clump.

After the needles were removed, the shoots were given 24 hours for sap to close over the scars. The sample needle clump was tagged for identification. Following several measurement sessions (generally over a few weeks), the tagged needles were collected, counted, and bagged for later determination of needle areas.

The true leaf surface area of each needle was calculated using the volume displacement technique described by Brand (1987). The true sample area was then used to correct the porometer conductance values as described in the porometer's manual.

1993 Experiment

Sampling in 1993 was designed to investigate the variability of stomatal conductance in the YJP forest within the tower WAB. Measurements were stratified according to needle age, position in the tree, and location in the forest. These subcanopies were selected to be representative of the range of canopy morphologies (tree height and spacing) within the WAB as determined from the analysis of tree size distribution (described above). The mean values of the three canopy parameters are summarized for each subcanopy below, where n/a means "not applicable":

Sub canopy	dbh (cm)	h (m)	stem density (trees/ha)
1	n/a	1.2	63000
2	3.65	3.7	8000
3	2.02	2.5	18000
4	n/a	1.2	78000
5	3.39	3.5	7000
6	1.96	2.5	15000

Three canopy parameters are encoded in the variable CANOPY_ID, a three-digit number. The first (left-most) digit of CANOPY_ID represents location in the forest. This single digit ranges from 1 to 6, representing six different locations or subcanopies within the WAB. The second digit represents needle age classification. A 0 represents current year needles, and a 1 represents all needles aged 1 year and greater. Finally, the third (right-most) digit represents position on the tree. This digit ranges from 0 to 3. A 0 represents breast height measurements regardless of subcanopy location. Digits of 1, 2, and 3 represent other height positions that are dependent upon subcanopy. For the small tree height canopies (locations 1 and 4), breast height was effectively the top of the trees. Thus, a position indicator of 1 represents a measurement of approximately 2/3 of the tree height down from the top of the canopy. In the taller canopies (locations 2, 3, 5, and 6), breast height represented the lowest position in the tree that was sampled. A position indicator of 2 represents approximately 1/2 to 2/3 the height of the tree from the ground. A position indicator of 3 indicates a measurement near the top of the canopy.

All porometry data are presented as the means from each porometry session. Sessions lasted between 15 and 30 minutes, and one to five sessions occurred on a given day.

1994 Experiment

At the conclusion of the experiment in 1993, the porometer was recalibrated and used again in 1994.

Examination of the 1993 conductance data set revealed no significant differences between the numerous categories. Therefore, it was decided that the measurement strategy should be simplified for 1994. Two areas were selected for sampling. The first, roughly 20 m x 20 m in size, was located 150 m from the flux tower at a bearing of 56°; it was considered to be representative of the majority of the site that was characterized by the presence of well-drained, sandy soil. A similar sized area was chosen 300 m from the flux tower at a bearing of 61° to represent the wetter eastern border zone of the site. In order to correspond with LAI measurements, conductance samples were stratified into two height classes: tall and short. A tall tree was >1.3 m and a short tree was <1.3 m in height. Samples were also classified as being above or below breast height. During a 30-minute sampling period, samples were collected from one or both sites, depending on the time required to establish an equilibrium condition in the sample chamber. For each site, in each sample period, 15 needle clumps were sampled: 5 clumps from short trees (below breast height), 5 clumps from tall trees above breast height, and 5 clumps from tall trees below breast height.

After several measurement sessions (generally over a few weeks), the tagged sample needle clumps were collected. The needles were removed from each sample and counted. Their projected area was determined by placing them on a light table and capturing their area and associated statistics (mean size and shape) with an AgVision imaging system (Decagon Devices, Pullman, WA, USA). The actual needle area was found by multiplying the projected area by 2.57, a species-specific correction factor. The correction factor was determined as the ratio of actual to projected needle area. Actual leaf area was found by volume displacement.

For each sample, the measured conductance represents a relative value that must be corrected for the actual needle area of each clump. This was accomplished by multiplying the relative conductance by the ratio of the aperture setting on the porometer (i.e., the needle area used by the porometer for its conductance measurement) to the actual needle area. It was assumed that needles which fell from the sample during measurements were of average area. The area of each sample was corrected for lost needles by adding the assumed area of lost needles (equal to the number of needles lost multiplied by the average needle area) to the area of that sample clump for all measurements taken prior to the loss of needles.

1996 Experiment

In 1996, the sample area for stomatal conductance was located approximately 30 m west of the flux tower and 10 m south of the soil moisture sampling array operated by the Hydrology (HYD)-01 group. The same sampling strategy used in 1994 was employed: each half-hour when data were collected, 15 trees were sampled, with 5 samples taken on needle clumps from tall trees above 1.3 m, 5 samples from tall trees below 1.3 m and 5 samples were located on small trees, each one being <1.3 m. The needle clumps were harvested at the same frequency as in 1994, and the same methodology was employed to find the actual leaf area of the sample.

LAI Measurements

LAI measurements were taken using two plant canopy analyzers (model LAI-2000, LI-COR, Inc., Lincoln, NE, USA). One unit, the rover, was positioned close to the ground to detect below-canopy readings at chosen sample points along the transects. The other unit was positioned permanently on top of the instrument hut, mounted on a tripod at a height approximately 4.75 m from the ground, and was operated in remote mode. This position provided an unobstructed view of the sky from well above the mean canopy height (approximately 2 to 3 meters). Above-canopy readings were recorded automatically every 15 seconds. The start and stop times for data collection were programmed by the operator.

Below-canopy measurements were taken near ground level, at a height of approximately 0.05 m, and at breast height (1.3 m) every 25 m along the 10 transects radial to the tower. To avoid underestimation of LAI from illuminated foliage in direct sunlight, measurements were taken just before sunrise and just after sunset. Sky conditions at these times were generally clear. Both sensors were fitted with a lens cap that restricted the field of view to 270°.

To ensure that the two LAI-2000 sensors were measuring the same light intensities, the units were intercalibrated. For calibration purposes, the sensors were placed side-by-side on the rooftop tripod, leveled, and exposed to the same ambient light conditions. The output of one of the sensors was then adjusted to ensure agreement between the light intensities measured by both sensors. In addition, the clocks on both units were synchronized to within <1 s of each other.

Each below-canopy measurement was stored as a separate data file. A single data file was created for the above-canopy readings. The data files from the two units were merged using LI-COR software (2000-90 Instrument Support Software v. 2.15, LI-COR, Inc., Lincoln, NE, USA), which matched each below-canopy reading with the above-canopy reading that was recorded at the closest time interval.

Since the LAI-2000 measures only projected leaf area, it was necessary to compute a correction factor to obtain the true LAI. Determination of the conifer correction factor (R') followed the methods of Gower and Norman (1991). Projected shoot area and total needle area were determined using a computer scanning and imaging system (AgVision, Decagon Devices, Pullman, WA, USA). Intact shoots were placed on the light table of the AgVision system. After determining the projected area, the shoot was turned 180° and the projected area was recalculated. The shoot projected area (PA(S)) was then determined by averaging these two values. The needles from the shoot were removed and measured to determine the total projected needle area (PA). R' was calculated from:

$$R' = PA / PA(S) \qquad (6.1)$$

R' varied with height on the tree as well as with tree size. Average values found were 2.17, 1.74, and 1.74 for 3-, 2-, and 1-m-tall trees. We also examined the shoot clumping factor (SCF) (Chen and Black, 1992; and Smith et al., 1993) and found an average value of 1.47 for the site.

A simple conversion factor was derived to convert the projected needle area (PA) measured by the AgVision imaging system to the actual needle area (based on the assumption that the geometry of jack pine (Pinus banksiana, Lamb.) is best represented by a half cylinder. The relationship is expressed as

$$AT = PA(1 + pi/2) * 2.57 \, PA \qquad (6.2)$$

where pi is 3.14, and AT is total needle area (cm^2).

The LAI found from destructive sampling of nine trees and expressed as one half the needle surface area per unit area was 1.50. Mean values of apparent LAI for all of the sample points on the 10 transects gave an overall site value of 0.79 ($\pm$ 0.27 s.d.). Using the site's SCF, the calculated actual LAI (one half-side only) is 1.16, which compares reasonably well with the measured LAI of 1.50.

6.2 Field Notes

Special Notes: 1993
All data were averaged over thirty minutes, starting on the hour and half-hour, and ending thirty minutes later. Sampling was continuous, and each day's data is from 0600 UTC to 0600 UTC the next day.
- LONGWAVE_IN_1138CM was calculated as a residual.
- Small nighttime values for SOLAR_RAD_IN_1182CM, SOLAR_RAD_OUT_1158CM,
- PPFD_IN_1154CM, and PPFD_OUT_1136CM were set to zero to account for very slight zero depressions and elevations in the radiometers.
- BIO_TEMP_SMALL_TREES is an average value calculated from the temperatures of the small trees at both the north and west sites.
- HEAT_STORAGE_TOTAL_AVERAGE is an average value calculated from the total heat storage calculated at both the north and west sites.
- HEAT_STORAGE_BIO_AVERAGE is an average value calculated from the biomass heat storage calculated at both the north and west sites.
- Data collection began on DAY 227 at 2330.

Special Notes: 1994
All data were averaged over thirty minutes, starting on the hour and half-hour, and ending thirty minutes later. Sampling was continuous and each day's data is from 0600 UTC to 0600 UTC the next day.
- LONGWAVE_IN_1138CM was calculated as a residual.
- Small nighttime values for SOLAR_RAD_IN_1182CM, SOLAR_RAD_OUT_1158CM, PPFD_IN_1154CM, and PPFD_OUT_1136CM were set to zero to account for very slight zero depressions and elevations in the radiometers.
- BIO_TEMP_SMALL_TREES is an average value found from the temperatures of the small trees at both the north and west sites.
- R_NET_1170CM_CORRECTED is calculated from day and night time equations taken from Hodges and Smith (1997) (see documentation for details).
- When SOLAR_RAD_IN_1182CM is greater than zero, CO2_TOTAL_FLUX_900CM is the sum of CO2_EDDY_FLUX_900CM and CO2_STORAGE_FLUX_900CM. If CO2_STORAGE_FLUX_900CM is missing, then CO2_EDDY_FLUX_900CM is used for CO2_TOTAL_FLUX_900CM.
- When SOLAR_RAD_IN_1182CM is equal to zero, CO2_TOTAL_FLUX_900CM is the sum of CO2_FLUX_NIGHT_MODEL_900CM and CO2_STORAGE_FLUX_900CM. If CO2_STORAGE_FLUX_900CM is missing, then CO2_FLUX_NIGHT_MODEL_900CM is used for CO2_TOTAL_FLUX_900CM.

Data Period: May 24 - June 6/94 (DOY 144-157)

- LONGWAVE_OUT_1138 sensor installed on DOY 148 at 1630
- SOIL_TEMP_NORTH_25CM, SOIL_TEMP_NORTH_50CM and SOIL_TEMP_NORTH_75CM thermocouples not installed until 179 at 2030.
- LATENT_HEAT_FLUX_900CM, SENSIBLE_HEAT_FLUX_900CM, H2O_FLUX_900CM, CO2_TOTAL_FLUX_900CM, CO2_CONC_900CM, SPECIFIC_HUMIDITY_900CM, SPECIFIC_HUMIDITY_STDEV_900CM, W_MEAN_900CM and W_STDEV_900CM values are missing on DOYs 144, 145, 147 from 1830-2230, 148 at 2030 through to 149 at 600 and 149 from 630-1530 due to weather and 153 from 2100-2130 due to lag tests.
- SOLAR_RAD_IN_1182CM, SOLAR_RAD_OUT_1158CM, NET_SOLAR_RAD_1170CM, LONGWAVE_IN_1138CM, TOTAL_RAD_IN_1160CM, TOTAL_RAD_OUT_1148CM, R_NET_1170CM, R_NET_1170CM_CORRECTED, PPFD_IN_1154CM, PPFD_OUT_1136CM, SURFACE_ALBEDO, SOIL_TEMP_NORTH_1CM, SOIL_TEMP_NORTH_5CM, SOIL_TEMP_NORTH_10CM, SOIL_TEMP_WEST_25CM, SOIL_TEMP_WEST_50CM, SOIL_TEMP_WEST_75CM, SOIL_TEMP_WEST_100CM, DRY_BULB_CANOPY_160CM,DRY_BULB_TEMP_517CM, DRY_BULB_TEMP_610CM, DRY_BULB_TEMP_715CM, DRY_BULB_TEMP_770CM, DRY_BULB_TEMP_1030CM, WET_BULB_CANOPY_160CM, WET_BULB_TEMP_517CM, WET_BULB_TEMP_610CM, WET_BULB_TEMP_715CM, WET_BULB_TEMP_770CM, WET_BULB_TEMP_1030CM, BIO_TEMP_SMALL_TREES, BIO_TEMP_MEDIUM_TREES, BIO_TEMP_LARGE_TREES, VAPOUR_PRESSURE_CANOPY_160CM, VAPOUR_PRESSURE_517CM, VAPOUR_PRESSURE_610CM, VAPOUR_PRESSURE_715CM, VAPOUR_PRESSURE_770CM, VAPOUR_PRESSURE_1030CM, WIND_SPEED_517CM, WIND_SPEED_610CM, WIND_SPEED_715CM, WIND_SPEED_770CM, WIND_SPEED_1030CM, WIND_DIR_1030CM, WIND_DIR_STDEV_1030CM and RAINFALL_250CM values are missing on DOYs 149 from 1530-2300 and 157 from 1500-1830.
- SOIL_HEAT_FLUX_NORTH_10CM, SOIL_HEAT_FLUX_WEST_10CM, HEAT_STORAGE_NORTH_TOTAL, HEAT_STORAGE_WEST_TOTAL, HEAT_STORAGE_NORTH_BIO, HEAT_STORAGE_WEST_BIO, HEAT_STORAGE_SENSIBLE_AIR, HEAT_STORAGE_LATENT_AIR, HEAT_STORAGE_NORTH_10CM and HEAT_STORAGE_WEST_10CM values are missing on DOYs 149 and 157.

Data Period: June 7 - June 20/94 (DOY 158-171)

- SOIL_TEMP_NORTH_25CM, SOIL_TEMP_NORTH_50CM and SOIL_TEMP_NORTH_75CM thermocouples not installed until 179 at 2030.
- LATENT_HEAT_FLUX_900CM, SENSIBLE_HEAT_FLUX_900CM, H2O_FLUX_900CM, CO2_TOTAL_FLUX_900CM, CO2_CONC_900CM, SPECIFIC_HUMIDITY_900CM, SPECIFIC_HUMIDITY_STDEV_900CM, W_MEAN_900CM and W_STDEV_900CM values are missing on DOY 162 from 1800-600, on 163, on 164 from 630-1500 and on 167 at 1900 through to 168 at 600 due to weather.
- SOLAR_RAD_IN_1182CM, SOLAR_RAD_OUT_1158CM, NET_SOLAR_RAD_1170CM, LONGWAVE_IN_1138CM, TOTAL_RAD_IN_1160CM, TOTAL_RAD_OUT_1148CM, R_NET_1170CM, R_NET_1170CM_CORRECTED, PPFD_IN_1154CM, PPFD_OUT_1136CM, SURFACE_ALBEDO, SOIL_TEMP_NORTH_1CM, SOIL_TEMP_NORTH_5CM, SOIL_TEMP_NORTH_10CM, SOIL_TEMP_WEST_25CM, SOIL_TEMP_WEST_50CM, SOIL_TEMP_WEST_75CM, SOIL_TEMP_WEST_100CM, DRY_BULB_CANOPY_160CM, DRY_BULB_TEMP_517CM, DRY_BULB_TEMP_610CM, DRY_BULB_TEMP_715CM, DRY_BULB_TEMP_770CM, DRY_BULB_TEMP_1030CM, WET_BULB_CANOPY_160CM, WET_BULB_TEMP_517CM, WET_BULB_TEMP_610CM, WET_BULB_TEMP_715CM,

WET_BULB_TEMP_770CM, WET_BULB_TEMP_1030CM,
BIO_TEMP_SMALL_TREES, BIO_TEMP_MEDIUM_TREES,
BIO_TEMP_LARGE_TREES, VAPOUR_PRESSURE_CANOPY_160CM,
VAPOUR_PRESSURE_517CM, VAPOUR_PRESSURE_610CM,
VAPOUR_PRESSURE_715CM, VAPOUR_PRESSURE_770CM,
VAPOUR_PRESSURE_1030CM, WIND_SPEED_517CM, WIND_SPEED_610CM,
WIND_SPEED_715CM, WIND_SPEED_770CM, WIND_SPEED_1030CM,
WIND_DIR_1030CM, WIND_DIR_STDEV_1030CM and RAINFALL_250CM values are
missing on 165 at 1500 through 166 at 600 and on 171 at 1900 through 172 at 600 due to
weather.
- SOIL_HEAT_FLUX_NORTH_10CM, SOIL_HEAT_FLUX_WEST_10CM,
HEAT_STORAGE_NORTH_TOTAL, HEAT_STORAGE_WEST_TOTAL,
HEAT_STORAGE_NORTH_BIO, HEAT_STORAGE_WEST_BIO,
HEAT_STORAGE_SENSIBLE_AIR, HEAT_STORAGE_LATENT_AIR,
HEAT_STORAGE_NORTH_10CM and HEAT_STORAGE_WEST_10CM values are
missing on DOYs 163, 165 and 171.

Data Period: June 21 - July 4/94 (DOY 172-185)
- SOIL_TEMP_NORTH_25CM, SOIL_TEMP_NORTH_50CM and
SOIL_TEMP_NORTH_75CM thermocouples not installed until 179 at 2030.
- LATENT_HEAT_FLUX_900CM, SENSIBLE_HEAT_FLUX_900CM,
H2O_FLUX_900CM, CO2_TOTAL_FLUX_900CM, CO2_CONC_900CM,
SPECIFIC_HUMIDITY_900CM, SPECIFIC_HUMIDITY_STDEV_900CM,
W_MEAN_900CM and W_STDEV_900CM values are missing from DOY 184 at 1500
through 189 at 2000 due to generator problems.
- WIND_DIR_1030CM sensor malfunction from DOY 172 through to 190 at 2330. Reinstalled
at 2400 on DOY 190. Consequently, no values of WIND_DIR_STDEV_1030CM.
- RAINFALL_250CM gauge malfunction on DOY 185 from 30-1900. Reinstalled at 1930 on
DOY 185.

Data Period: July 5 - July 18/94 (DOY 186-199)
- LATENT_HEAT_FLUX_900CM, SENSIBLE_HEAT_FLUX_900CM,
H2O_FLUX_900CM, CO2_TOTAL_FLUX_900CM, CO2_CONC_900CM,
SPECIFIC_HUMIDITY_900CM, SPECIFIC_HUMIDITY_STDEV_900CM,
W_MEAN_900CM and W_STDEV_900CM values are missing from DOY 184 at 1500
through 189 at 2000 due to generator problems. There are no readings on DOYs 191 at 2200
through to 192 at 1730, on 193 at 1600 through to 195 at 2100 and on 196 from 1500-1730
due to weather.
- SOIL_HEAT_FLUX_NORTH_10CM, SOIL_HEAT_FLUX_WEST_10CM,
HEAT_STORAGE_NORTH_TOTAL, HEAT_STORAGE_WEST_TOTAL,
HEAT_STORAGE_NORTH_BIO, HEAT_STORAGE_WEST_BIO,
HEAT_STORAGE_SENSIBLE_AIR, HEAT_STORAGE_LATENT_AIR,
HEAT_STORAGE_NORTH_10CM and HEAT_STORAGE_WEST_10CM values are
missing on DOY 190.
- WIND_DIR_1030CM sensor malfunction from DOY 172 through to 190 at 2330. Reinstalled
at 2400 on DOY 190. Consequently, no values of WIND_DIR_STDEV_1030CM.

Data Period: July 19 - August 1/94 (DOY 200-213)
- LATENT_HEAT_FLUX_900CM, SENSIBLE_HEAT_FLUX_900CM, H2O_FLUX_900CM, CO2_TOTAL_FLUX_900CM, CO2_CONC_900CM, SPECIFIC_HUMIDITY_900CM, SPECIFIC_HUMIDITY_STDEV_900CM, W_MEAN_900CM and W_STDEV_900CM values are missing on DOYs 200 at 1500 through, 201 at 1730 due to instrument malfunction, on DOY 203 from 1230-1530 due to weather and on DOY 204 from 230-400 due to data inconsistencies. On DOY 206 from 1330-1530 and from 1830-1930 due to data inconsistencies and on DOY 207 at 1300 and on DOY 208 from 230-300 due to data inconsistencies.

Data Period: August 2 - August 15/94 (DOY 214-227)
- LATENT_HEAT_FLUX_900CM, SENSIBLE_HEAT_FLUX_900CM, H2O_FLUX_900CM, CO2_TOTAL_FLUX_900CM, CO2_CONC_900CM, SPECIFIC_HUMIDITY_900CM, SPECIFIC_HUMIDITY_STDEV_900CM, W_MEAN_900CM and W_STDEV_900CM values are missing on DOYs 217 at 2330 through, 218 at 1930, 223 at 2100 through 225 at 1530 due to weather. On DOY 227 at 2400 through 228 at 100 due to data inconsistencies.

Data Period: August 16 - August 29/94 (DOY 228-241)
- LATENT_HEAT_FLUX_900CM, SENSIBLE_HEAT_FLUX_900CM, H2O_FLUX_900CM, CO2_TOTAL_FLUX_900CM, CO2_CONC_900CM, SPECIFIC_HUMIDITY_900CM, SPECIFIC_HUMIDITY_STDEV_900CM, W_MEAN_900CM and W_STDEV_900CM values are missing on DOYs 234 at 130 through 235 at 1600, 239 at 1430 through 240 at 1430 due to instrument malfunction. On DOYs 241 at 1730 through 242 at 1430 due to weather.
- SOIL_TEMP_WEST_5CM sensor unreliable on DOYs 237 at 2030 through 238 at 230, on DOY 238 from 730-1030, on DOY 240 from 630-930, on DOY 241 at 700 through 242 at 600 due to wet conditions.

Data Period: August 30 - September 12/94 (DOY 242-255)
- LATENT_HEAT_FLUX_900CM, SENSIBLE_HEAT_FLUX_900CM, H2O_FLUX_900CM, CO2_TOTAL_FLUX_900CM, CO2_CONC_900CM, SPECIFIC_HUMIDITY_900CM, SPECIFIC_HUMIDITY_STDEV_900CM, W_MEAN_900CM and W_STDEV_900CM values are missing on Jdays 242 from 630-1430, 247 at 1430 through 248 at 1700 due to weather.
- LATENT_HEAT_FLUX_900CM and CO2_TOTAL_FLUX_900CM have missing values on Jdays 253 at 130 through 254 at 600 and on 255 from 630-1500 due to data inconsistency.
- SOIL_TEMP_WEST_5CM sensor unreliable on Jdays 242 from 630-1630, on Jday 248 at 1600 through 249 at 900, on Jday 249 from 1930-2200, on Jday 250 at 2030 through 251 at 230, on Jday 251 from 600-1100, on Jday 251 at 1800 through 252 at 1500, on Jday 252 at 1630 through 253 at 1830, on Jday 255 from 1530-1730, on Jday 255 at 1930 through 256 at 600 due to wet conditions.

Data Period: September 13 - September 20/94 (DOY 256-263)
- LATENT_HEAT_FLUX_900CM, SENSIBLE_HEAT_FLUX_900CM, H2O_FLUX_900CM, CO2_TOTAL_FLUX_900CM, CO2_CONC_900CM, SPECIFIC_HUMIDITY_900CM, SPECIFIC_HUMIDITY_STDEV_900CM, W_MEAN_900CM and W_STDEV_900CM values are missing on DOYs 256 from 1630-1700, and 257 from 1630-1700 due to weather. On 258 from 730-1500 and on 259 from 630-1600 due to instrument malfunction. On DOY 263 at 1530 through 264 at 600 due to the end of the 1994 field season.
- SOLAR_RAD_IN_1182CM, SOLAR_RAD_OUT_1158CM, NET_SOLAR_RAD_1170CM, LONGWAVE_IN_1138CM, TOTAL_RAD_IN_1160CM, TOTAL_RAD_OUT_1148CM, R_NET_1170CM, R_NET_1170CM_CORRECTED, PPFD_IN_1154CM,

PPFD_OUT_1136CM, SURFACE_ALBEDO, SOIL_TEMP_NORTH_1CM, SOIL_TEMP_NORTH_5CM, SOIL_TEMP_NORTH_10CM, SOIL_TEMP_WEST_25CM, SOIL_TEMP_WEST_50CM, SOIL_TEMP_WEST_75CM, SOIL_TEMP_WEST_100CM, DRY_BULB_CANOPY_160CM, DRY_BULB_TEMP_517CM, DRY_BULB_TEMP_610CM, DRY_BULB_TEMP_715CM, DRY_BULB_TEMP_770CM, DRY_BULB_TEMP_1030CM, WET_BULB_CANOPY_160CM, WET_BULB_TEMP_517CM, WET_BULB_TEMP_610CM, WET_BULB_TEMP_715CM, WET_BULB_TEMP_770CM, WET_BULB_TEMP_1030CM, BIO_TEMP_SMALL_TREES, BIO_TEMP_MEDIUM_TREES, BIO_TEMP_LARGE_TREES, VAPOUR_PRESSURE_CANOPY_160CM, VAPOUR_PRESSURE_517CM, VAPOUR_PRESSURE_610CM, VAPOUR_PRESSURE_715CM, VAPOUR_PRESSURE_770CM, VAPOUR_PRESSURE_1030CM, WIND_SPEED_517CM, WIND_SPEED_610CM, WIND_SPEED_715CM, WIND_SPEED_770CM, WIND_SPEED_1030CM, WIND_DIR_1030CM, WIND_DIR_STDEV_1030CM and RAINFALL_250CM values are missing on DOY 263 at 1530 through 264 at 600 due to the end of the 1994 field season.

- SOIL_HEAT_FLUX_NORTH_10CM, SOIL_HEAT_FLUX_WEST_10CM, HEAT_STORAGE_NORTH_TOTAL, HEAT_STORAGE_WEST_TOTAL, HEAT_STORAGE_NORTH_BIO, HEAT_STORAGE_WEST_BIO, HEAT_STORAGE_SENSIBLE_AIR, HEAT_STORAGE_LATENT_AIR, HEAT_STORAGE_NORTH_10CM and HEAT_STORAGE_WEST_10CM values are missing on DOYs 262 and 263.
- SOIL_TEMP_WEST_5CM sensor unreliable on DOYs 256 from 630-1130, on DOY 256 at 1600 through 257 at 600, on DOY 258 from 500-800, on DOY 258 at 1530 through 259 at 800, on DOY 259 from 1230-1530, on DOY 259 from 1800-2200 due to wet conditions.

Special Notes: 1996

All data were averaged over thirty-minute intervals, starting on the hour or half-hour, and ending thirty minutes later. Sampling was continous, and each day's data is from 0600 UTC to 0600 UTC the next day.

- LONGWAVE_IN_1138CM was calculated as a residual.
- Small nighttime values for SOLAR_RAD_IN_1182CM, SOLAR_RAD_OUT_1158CM, PPFD_IN_1154CM, and PPFD_OUT_1136CM were set to zero to account for very slight zero depressions and elevations in the radiometers.
- BIO_TEMP_SMALL_TREES is an average value found from the temperatures of the small trees at both the north and west sites.
- R_NET_1170CM_CORRECTED was calculated from day and night time equations developed by Hodges and Smith (1997) (see documentation for details).
- When SOLAR_RAD_IN_1182CM is greater than zero, CO2_TOTAL_FLUX_900CM is the sum of CO2_EDDY_FLUX_900CM AND CO2_STORAGE_FLUX_900CM. If CO2_STORAGE_FLUX_900CM is missing, then CO2_EDDY_FLUX_900CM is used for CO2_TOTAL_FLUX_900CM.
- When SOLAR_RAD_IN_1182CM is equal to zero, CO2_TOTAL_FLUX_900CM is the sum of CO2_FLUX_NIGHT_MODEL_900CM and CO2_STORAGE_FLUX_900CM. If CO2_STORAGE_FLUX_900CM is missing, then CO2_FLUX_NIGHT_MODEL_900CM is used for CO2_TOTAL_FLUX_900CM.

Data Period: May 8\96 - July 3\96 (DOY 129-185)

- HEAT_STORAGE_NORTH_10CM and HEAT_STORAGE_WEST_10CM values are missing from DOY 129 to DOY 178 (inclusive) because soil moisture data were not available.
- HEAT_STORAGE_LATENT_AIR is missing DOY 129-133(2030), 137(1400)-141(1700), and 179(1430-2130). HEAT_STORAGE_TOTAL_NORTH and HEAT_STORAGE_TOTAL_WEST are therefore calculated from the remaining heat storage variables.

Data Period: August 15 - August 28\96 (DOY 228-241)
- Values for SOIL_TEMP_NORTH_1CM, SOIL_TEMP_NORTH_5CM, SOIL_TEMP_NORTH_10CM, SOIL_TEMP_NORTH_25CM, SOIL_TEMP_NORTH_50CM, SOIL_TEMP_NORTH_75CM, SOIL_TEMP_WEST_1CM, SOIL_TEMP_WEST_5CM, SOIL_TEMP_WEST_10CM, SOIL_TEMP_WEST_25CM, SOIL_TEMP_WEST_50CM, SOIL_TEMP_WEST_75CM, SOIL_TEMP_WEST_100CM, and
- RAINFALL_250CM were interpolated on DOY 232 at 1630.

Data Period: October 10 - October 23\96 (DOY 284-297)
- WIND_SPEED_517CM, WIND_SPEED_770CM, WIND_SPEED_1030CM, WIND_DIR_1030CM, and WIND_DIR_STDEV_1030CM values are missing on DOY 289(2000-0600), 290, 291, and 292 (0630-1800) because of freezing of the sensors.

Data Period: October 24 - November 6\96 (DOY 298-311)
- WIND_SPEED_517CM, WIND_SPEED_770CM, and WIND_SPEED_1030CM values are missing on DOY 300(0500-0600), 301, 302, and 303(0630-2030) because of freezing of the anemometers.

7. Data Description

7.1 Spatial Characteristics

7.1.1 Spatial Coverage
All data were collected at the BOREAS NSA-YJP site. North American Datum of 1983 (NAD83) coordinates for the site are latitude 55.89575° N, longitude 98.28706° W, and elevation of 249.29 m. The prevailing wind direction in the area is from the west. Therefore, the access path to the tower and all of the hard services (generator, fuel storage area, instrument hut, and storage tent) were located east of the tower.

Porometric data were collected at two locations on the YJP site in 1994. One location was designated as "dry" because it was located on the dry, sandy soil near the flux tower, and the other location was designated as "wet" because it was located on the wetter part of the site east of the flux tower. The wet site was 290 m from the tower at a bearing of 61 degrees, and the dry site was 150 m from the tower at a bearing of 56 degrees. The strategy of choosing two sample positions was to see whether the clearly different soil moisture status of the sites influenced the behavior of stomatal conductance. In 1996, one porometric sample zone was located approximately 40 m from the tower at a bearing of 250 degrees. This site was chosen in order to be close to the dense array of continuous soil moisture sample profiles run by HYD-01.

7.1.2 Spatial Coverage Map
Not applicable.

7.1.3 Spatial Resolution
The data collected from towers are usually thought of as point data. However, they actually represent an integrated response to the surface/atmosphere interaction, especially in terms of the eddy flux data, which are considered to represent an integrated upwind surface source region (Leclerc and Thurtell, 1990; Schmid and Oke, 1990). In general, at the YJP the fluxes apply to the surface between 20 to 400 meters upwind. At the fen, where fetch in certain wind directions is limited, data uncertainties may occur (see Section 10.1).

7.1.4 Projection
Not applicable.

7.1.5 Grid Description
Not applicable.

7.2 Temporal Characteristics

7.2.1 Temporal Coverage
The start and stop times for the experiments were as follows:

15-Aug-1993 to 31-Aug-1993
25-May-1994 to 19-Sep-1994
30-Apr-1996 to 15-Nov-1996

7.2.2 Temporal Coverage Map
Not applicable.

7.2.3 Temporal Resolution
With one exception, the data values submitted to BORIS were integrations of the conditions for the 30-minute reporting periods. The exception is the porometric data, and specifically the stomatal conductance of the jack pine, which is submitted as shorter-term averages.

Meteorological data were output at 15- and 30-minute intervals depending upon the variable. The 15-minute data included only absolute wet- and dry-bulb air temperatures and soil temperatures, which were used for heat storage calculations (described below). All signals, except temperature differences, were averaged over 30-minute periods. Only the 30-minute data were reported to BORIS. Eddy covariance data were output every 30 minutes.

Porometry data and other biophysical measurements were conducted at irregular sampling intervals as conditions and resources permitted. Dates and times are noted in the data submissions.

7.3 Data Characteristics
The data provided by the TF-10 team consist of both tower flux and porometry measurements. The details of these two data sets are contained in the following sections.

7.3.1 Parameter/Variable
The parameters contained in the flux data files on the CD-ROM are:

```
        Column Name
--------------------------------
SITE_NAME
SUB_SITE
DATE_OBS
TIME_OBS
SENSIBLE_HEAT_FLUX_ABV_CNPY
LATENT_HEAT_FLUX_ABV_CNPY
NET_RAD_ABV_CNPY
CO2_FLUX_ABV_CNPY
CO2_CONC_ABV_CNPY
CO2_STORAGE
CO2_FLUX_ABV_PLUS_STORAGE
NIGHT_CO2_FLUX_ABV_CNPY
DOWN_PPFD_ABV_CNPY
UP_PPFD_ABV_CNPY
WIND_SPEED_510CM
WIND_SPEED_517CM
WIND_SPEED_610CM
WIND_SPEED_710CM
```

```
WIND_SPEED_715CM
WIND_SPEED_770CM
WIND_SPEED_910CM
WIND_SPEED_ABV_CNPY
MEAN_WIND_DIR_MAG_ABV_CNPY
SDEV_WIND_DIR_MAG_ABV_CNPY
AIR_TEMP_ABV_CNPY
H2O_FLUX_ABV_CNPY
SOIL_HEAT_FLUX_NORTH_10CM
SOIL_HEAT_FLUX_WEST_10CM
SOIL_TEMP_NORTH_1CM
SOIL_TEMP_NORTH_5CM
SOIL_TEMP_NORTH_10CM
SOIL_TEMP_NORTH_25CM
SOIL_TEMP_NORTH_50CM
SOIL_TEMP_NORTH_75CM
SOIL_TEMP_WEST_1CM
SOIL_TEMP_WEST_5CM
SOIL_TEMP_WEST_10CM
SOIL_TEMP_WEST_25CM
SOIL_TEMP_WEST_50CM
SOIL_TEMP_WEST_75CM
SOIL_TEMP_WEST_100CM
RAINFALL
DOWN_SOLAR_RAD_ABV_CNPY
UP_SOLAR_RAD_ABV_CNPY
NET_SOLAR_RAD_ABV_CNPY
DOWN_TOTAL_RAD_ABV_CNPY
UP_TOTAL_RAD_ABV_CNPY
AIR_TEMP_510CM
AIR_TEMP_517CM
AIR_TEMP_610CM
AIR_TEMP_710CM
AIR_TEMP_715CM
AIR_TEMP_770CM
AIR_TEMP_910CM
WET_BULB_TEMP_510CM
WET_BULB_TEMP_517CM
WET_BULB_TEMP_610CM
WET_BULB_TEMP_710CM
WET_BULB_TEMP_715CM
WET_BULB_TEMP_770CM
WET_BULB_TEMP_910CM
WET_BULB_TEMP_ABV_CNPY
VAPOR_PRESS_510CM
VAPOR_PRESS_517CM
VAPOR_PRESS_610CM
VAPOR_PRESS_710CM
VAPOR_PRESS_715CM
VAPOR_PRESS_770CM
VAPOR_PRESS_910CM
VAPOR_PRESS_ABV_CNPY
SURF_PRESS
DOWN_LONGWAVE_RAD_ABV_CNPY
```

```
UP_LONGWAVE_RAD_ABV_CNPY
CORR_NET_RAD_ABV_CNPY
ALBEDO
CNPY_AIR_TEMP_160CM
CNPY_WET_BULB_TEMP_160CM
CNPY_VAPOR_PRESS_160CM
MEAN_SMALL_TREE_BIOMASS_TEMP
MEAN_MEDIUM_TREE_BIOMASS_TEMP
MEAN_LARGE_TREE_BIOMASS_TEMP
TOTAL_HEAT_STORAGE_NORTH
TOTAL_HEAT_STORAGE_WEST
MEAN_TOTAL_HEAT_STORAGE
BIO_HEAT_STORAGE_NORTH
BIO_HEAT_STORAGE_WEST
MEAN_BIO_HEAT_STORAGE
SENSIBLE_AIR_HEAT_STORAGE
LATENT_AIR_HEAT_STORAGE
SOIL_HEAT_STORAGE_NORTH_10CM
SOIL_HEAT_STORAGE_WEST_10CM
MEAN_SPECIFIC_HUM_ABV_CNPY
SDEV_SPECIFIC_HUM_ABV_CNPY
MEAN_W_WIND_SPEED_ABV_CNPY
SDEV_W_WIND_SPEED_ABV_CNPY
REL_HUM_ABV_CNPY
CRTFCN_CODE
REVISION_DATE
```

The parameters contained in the porometry data files on the CD-ROM are:

```
           Column Name
------------------------------
SITE_NAME
SUB_SITE
DATE_OBS
TIME_OBS
TREE_HT_CLASS
MEASUREMENT_HT_CLASS
STOMATAL_CONDUCT_H2O
CRTFCN_CODE
REVISION_DATE
```

7.3.2 Variable Description/Definition
The descriptions of the parameters contained in the flux data files on the CD-ROM are:

```
         Column Name                         Description
------------------------------   -------------------------------------------------
SITE_NAME                        The identifier assigned to the site by BOREAS,
                                 in the format SSS-TTT-CCCCC, where SSS identifies
                                 the portion of the study area: NSA, SSA, REG,
                                 TRN, and TTT identifies the cover type for the
                                 site, 999 if unknown, and CCCCC is the identifier
                                 for site, exactly what it means will vary with
                                 site type.
SUB_SITE                         The identifier assigned to the sub-site by BOREAS
```

	in the format GGGGG-IIIII, where GGGGG is the group associated with the sub-site instrument, e.g. HYD06 or STAFF, and IIIII is the identifier for sub-site, often this will refer to an instrument.
DATE_OBS	The date on which the data were collected.
TIME_OBS	The Greenwich Mean Time (GMT) of the start of the data collection.
SENSIBLE_HEAT_FLUX_ABV_CNPY	The sensible heat flux measured above the canopy.
LATENT_HEAT_FLUX_ABV_CNPY	The latent heat flux measured above the canopy.
NET_RAD_ABV_CNPY	The net radiation measured above the canopy.
CO2_FLUX_ABV_CNPY	The carbon dioxide flux measured above the canopy.
CO2_CONC_ABV_CNPY	The carbon dioxide concentration measured above the canopy.
CO2_STORAGE	The storage term of carbon dioxide under the eddy flux system.
CO2_FLUX_ABV_PLUS_STORAGE	The sum of the above canopy carbon dioxide flux and the under flux instrument storage term.
NIGHT_CO2_FLUX_ABV_CNPY	The nighttime carbon dioxide flux estimated from a model based on temperature.
DOWN_PPFD_ABV_CNPY	The downward (incoming) photosynthetic photon flux density measured above the canopy.
UP_PPFD_ABV_CNPY	The reflected photosynthetic photon flux density measured above the canopy.
WIND_SPEED_510CM	The wind speed measured 5.1 m above the ground.
WIND_SPEED_517CM	The wind speed measured 5.17 m above the ground.
WIND_SPEED_610CM	The wind speed measured 6.1 m above the ground.
WIND_SPEED_710CM	The wind speed measured 7.1 m above the ground.
WIND_SPEED_715CM	The wind speed measured 7.15 m above the ground.
WIND_SPEED_770CM	The wind speed measured 7.7 m above the ground.
WIND_SPEED_910CM	The wind speed measured 9.1 m above the ground.
WIND_SPEED_ABV_CNPY	The wind speed measured above the canopy.
MEAN_WIND_DIR_MAG_ABV_CNPY	The average wind direction in relation to magnetic north, over 30 minutes measured above the canopy.
SDEV_WIND_DIR_MAG_ABV_CNPY	The standard deviation of the wind direction in relation to magnetic north, over 30 minutes measured above the canopy.
AIR_TEMP_ABV_CNPY	The air temperature measured above the canopy.
H2O_FLUX_ABV_CNPY	The water vapor flux measured above the canopy.
SOIL_HEAT_FLUX_NORTH_10CM	The soil heat flux measured 10 cm below the soil surface at a location north of the flux tower.
SOIL_HEAT_FLUX_WEST_10CM	The soil heat flux measured 10 cm below the soil surface at a location west of the flux tower.
SOIL_TEMP_NORTH_1CM	Soil temperature 1 cm below the soil surface at a location north of the flux tower.
SOIL_TEMP_NORTH_5CM	Soil temperature 5 cm below the soil surface at a location north of the flux tower.
SOIL_TEMP_NORTH_10CM	Soil temperature 10 cm below the soil surface at a location north of the flux tower.
SOIL_TEMP_NORTH_25CM	Soil temperature 25 cm below the soil surface at a location north of the flux tower.
SOIL_TEMP_NORTH_50CM	Soil temperature 50 cm below the soil surface at

	a location north of the flux tower.
SOIL_TEMP_NORTH_75CM	Soil temperature 75 cm below the soil surface at a location north of the flux tower.
SOIL_TEMP_WEST_1CM	Soil temperature 1 cm below the soil surface at a location west of the flux tower.
SOIL_TEMP_WEST_5CM	Soil temperature 5 cm below the soil surface at a location west of the flux tower.
SOIL_TEMP_WEST_10CM	Soil temperature 10 cm below the soil surface at a location west of the flux tower.
SOIL_TEMP_WEST_25CM	Soil temperature 25 cm below the soil surface at a location west of the flux tower.
SOIL_TEMP_WEST_50CM	Soil temperature 50 cm below the soil surface at a location west of the flux tower.
SOIL_TEMP_WEST_75CM	Soil temperature 75 cm below the soil surface at a location west of the flux tower.
SOIL_TEMP_WEST_100CM	Soil temperature 1 m below the soil surface at a location west of the flux tower.
RAINFALL	The amount of rainfall measured above the canopy in the 30 minute period following the given time.
DOWN_SOLAR_RAD_ABV_CNPY	The downward (incoming) solar radiation measured above the canopy.
UP_SOLAR_RAD_ABV_CNPY	The reflected (outgoing) solar radiation measured above the canopy.
NET_SOLAR_RAD_ABV_CNPY	The net solar radiation measured above the canopy.
DOWN_TOTAL_RAD_ABV_CNPY	The total downward (incoming) radiation measured above the canopy.
UP_TOTAL_RAD_ABV_CNPY	The total upward (outgoing) radiation measured above the canopy.
AIR_TEMP_510CM	The air temperature measured at 5.1 meters above the ground.
AIR_TEMP_517CM	The air temperature measured at 5.17 meters above the ground.
AIR_TEMP_610CM	The air temperature measured at 6.1 meters above the ground.
AIR_TEMP_710CM	The air temperature measured at 7.1 meters above the ground.
AIR_TEMP_715CM	The air temperature measured at 7.15 meters above the ground.
AIR_TEMP_770CM	The air temperature measured at 7.7 meters above the ground.
AIR_TEMP_910CM	The air temperature measured at 9.1 meters above the ground.
WET_BULB_TEMP_510CM	The wet bulb temperature measured at 5.1 meters above the ground.
WET_BULB_TEMP_517CM	The wet bulb temperature measured at 5.17 meters above the ground.
WET_BULB_TEMP_610CM	The wet bulb temperature measured at 6.1 meters above the ground.
WET_BULB_TEMP_710CM	The wet bulb temperature measured at 7.1 meters above the ground.
WET_BULB_TEMP_715CM	The wet bulb temperature measured at 7.15 meters above the ground.
WET_BULB_TEMP_770CM	The wet bulb temperature measured at 7.7 meters

	above the ground.
WET_BULB_TEMP_910CM	The wet bulb temperature measured at 9.1 meters above the ground.
WET_BULB_TEMP_ABV_CNPY	The wet bulb temperature measured above the canopy.
VAPOR_PRESS_510CM	The vapor pressure measured at 5.1 meters above the ground.
VAPOR_PRESS_517CM	The vapor pressure measured at 5.17 meters above the ground.
VAPOR_PRESS_610CM	The vapor pressure measured at 6.1 meters above the ground.
VAPOR_PRESS_710CM	The vapor pressure measured at 7.1 meters above the ground.
VAPOR_PRESS_715CM	The vapor pressure measured at 7.15 meters above the ground.
VAPOR_PRESS_770CM	The vapor pressure measured at 7.7 meters above the ground.
VAPOR_PRESS_910CM	The vapor pressure measured at 9.1 meters above the ground.
VAPOR_PRESS_ABV_CNPY	The vapor pressure measured above the canopy.
SURF_PRESS	The atmospheric pressure measured at the station.
DOWN_LONGWAVE_RAD_ABV_CNPY	The downward (incoming) longwave radiation measured above the canopy.
UP_LONGWAVE_RAD_ABV_CNPY	The upward (outgoing) longwave radiation measured above the canopy.
CORR_NET_RAD_ABV_CNPY	The corrected net radiation measured above the canopy, using equations developed by Hodges and Smith (1997).
ALBEDO	Surface solar albedo.
CNPY_AIR_TEMP_160CM	The air temperature in the canopy measured at 1.6 meters above the ground.
CNPY_WET_BULB_TEMP_160CM	The wet bulb temperature in the canopy measured at 1.6 meters above the ground.
CNPY_VAPOR_PRESS_160CM	The vapor pressure in the canopy measured at 1.6 meters above the ground.
MEAN_SMALL_TREE_BIOMASS_TEMP	The temperature of tree biomass in small trees. Measured using thermocouples embedded directly into the boles, 1/3 of the way up the tree and 1/3 of the radius into the boles. Three trees under 1.5 m height were measured.
MEAN_MEDIUM_TREE_BIOMASS_TEMP	The temperature of tree biomass in medium trees. Measured using thermocouples embedded directly into the boles, 1/3 of the way up the tree and 1/3 of the radius into the boles. Three trees over 2.5 m height were measured.
MEAN_LARGE_TREE_BIOMASS_TEMP	The temperature of tree biomass in large trees. Measured using thermocouples embedded directly into the boles, 1/3 of the way up the tree and 1/3 of the radius into the boles. Three trees over 5 m height were measured.
TOTAL_HEAT_STORAGE_NORTH	Total of minor heat storage terms including soil heat flux, storage in soil above flux plate, storage in biomass, and sensible and latent heat storage in the air at a location north of the

```
                                   flux tower.
TOTAL_HEAT_STORAGE_WEST            Total of minor heat storage terms including soil
                                   heat flux, storage in soil above flux plate,
                                   storage in biomass, and sensible and latent heat
                                   storage in the air at a location west of the flux
                                   tower.
MEAN_TOTAL_HEAT_STORAGE            Average of the north and west site total heat
                                   storage values.
BIO_HEAT_STORAGE_NORTH             Biomass heat storage for a site north of the flux
                                   tower.
BIO_HEAT_STORAGE_WEST              Biomass heat storage for a site west of the flux
                                   tower.
MEAN_BIO_HEAT_STORAGE              Average of the north and west site biomass heat
                                   storage values.
SENSIBLE_AIR_HEAT_STORAGE          Sensible heat storage in air column between the
                                   surface and net pyrradiometer.
LATENT_AIR_HEAT_STORAGE            Latent heat storage in air column between the
                                   surface and net pyrradiometer.
SOIL_HEAT_STORAGE_NORTH_10CM       Heat storage in the 10 cm of soil above the heat
                                   flux plate at a location north of the flux tower
SOIL_HEAT_STORAGE_WEST_10CM        Heat storage in the 10 cm of soil above the heat
                                   flux plate at a location west of the flux tower
MEAN_SPECIFIC_HUM_ABV_CNPY         The 30 minute mean specific humidity measured
                                   above the canopy.
SDEV_SPECIFIC_HUM_ABV_CNPY         The 30 minute standard deviation of specific
                                   humidity measured above the canopy.
MEAN_W_WIND_SPEED_ABV_CNPY         The 30 minute mean of the vertical wind speed
                                   measured above the canopy.
SDEV_W_WIND_SPEED_ABV_CNPY         The 30 minute standard deviation of the vertical
                                   wind speed measured above the canopy.
REL_HUM_ABV_CNPY                   The relative humidity measured above the canopy.
CRTFCN_CODE                        The BOREAS certification level of the data.
                                   Examples are CPI (Checked by PI), CGR (Certified
                                   by Group), PRE (Preliminary), and CPI-??? (CPI
                                   but questionable).
REVISION_DATE                      The most recent date when the information in the
                                   referenced data base table record was revised.
```

The descriptions of the parameters contained in the porometry data files on the CD-ROM are:

```
        Column Name                              Description
-----------------------------    --------------------------------------------------
SITE_NAME                        The identifier assigned to the site by BOREAS,
                                 in the format SSS-TTT-CCCCC, where SSS identifies
                                 the portion of the study area: NSA, SSA, REG,
                                 TRN, and TTT identifies the cover type for the
                                 site, 999 if unknown, and CCCCC is the identifier
                                 for site, exactly what it means will vary with
                                 site type.
SUB_SITE                         The identifier assigned to the sub-site by BOREAS
                                 in the format GGGGG-IIIII, where GGGGG is the
                                 group associated with the sub-site instrument,
                                 e.g. HYD06 or STAFF, and IIIII is the identifier
                                 for sub-site, often this will refer to an
```

```
                                        instrument.
DATE_OBS                                The date on which the data were collected.
TIME_OBS                                The Greenwich Mean Time (GMT) when the data were
                                        collected.
TREE_HT_CLASS                           The height class of the tree being measured.
MEASUREMENT_HT_CLASS                    The height class in the tree where the
                                        measurement was made.
STOMATAL_CONDUCT_H2O                    Stomatal conductance of water vapor.
CRTFCN_CODE                             The BOREAS certification level of the data.
                                        Examples are CPI (Checked by PI), CGR (Certified
                                        by Group), PRE (Preliminary), and CPI-??? (CPI
                                        but questionable).
REVISION_DATE                           The most recent date when the information in the
                                        referenced data base table record was revised.
```

7.3.3 Unit of Measurement
The measurement units for the parameters contained in the flux data files on the CD-ROM are:

```
        Column Name                                     Units
-------------------------------    -------------------------------------------------
SITE_NAME                          [none]
SUB_SITE                           [none]
DATE_OBS                           [DD-MON-YY]
TIME_OBS                           [HHMM GMT]
SENSIBLE_HEAT_FLUX_ABV_CNPY        [Watts][meter^-2]
LATENT_HEAT_FLUX_ABV_CNPY          [Watts][meter^-2]
NET_RAD_ABV_CNPY                   [Watts][meter^-2]
CO2_FLUX_ABV_CNPY                  [micromoles][meter^-2][second^-1]
CO2_CONC_ABV_CNPY                  [parts per million]
CO2_STORAGE                        [micromoles][meter^-2][second^-1]
CO2_FLUX_ABV_PLUS_STORAGE          [micromoles][meter^-2][second^-1]
NIGHT_CO2_FLUX_ABV_CNPY            [micromoles][meter^-2][second^-1]
DOWN_PPFD_ABV_CNPY                 [micromoles][meter^-2][second^-1]
UP_PPFD_ABV_CNPY                   [micromoles][meter^-2][second^-1]
WIND_SPEED_510CM                   [meters][second^-1]
WIND_SPEED_517CM                   [meters][second^-1]
WIND_SPEED_610CM                   [meters][second^-1]
WIND_SPEED_710CM                   [meters][second^-1]
WIND_SPEED_715CM                   [meters][second^-1]
WIND_SPEED_770CM                   [meters][second^-1]
WIND_SPEED_910CM                   [meters][second^-1]
WIND_SPEED_ABV_CNPY                [meters][second^-1]
MEAN_WIND_DIR_MAG_ABV_CNPY         [degrees from magnetic north]
SDEV_WIND_DIR_MAG_ABV_CNPY         [degrees from magnetic north]
AIR_TEMP_ABV_CNPY                  [degrees Celsius]
H2O_FLUX_ABV_CNPY                  [millimoles][meter^-2][second^-1]
SOIL_HEAT_FLUX_NORTH_10CM          [Watts][meter^-2]
SOIL_HEAT_FLUX_WEST_10CM           [Watts][meter^-2]
SOIL_TEMP_NORTH_1CM                [degrees Celsius]
SOIL_TEMP_NORTH_5CM                [degrees Celsius]
SOIL_TEMP_NORTH_10CM               [degrees Celsius]
SOIL_TEMP_NORTH_25CM               [degrees Celsius]
SOIL_TEMP_NORTH_50CM               [degrees Celsius]
SOIL_TEMP_NORTH_75CM               [degrees Celsius]
```

```
SOIL_TEMP_WEST_1CM              [degrees Celsius]
SOIL_TEMP_WEST_5CM              [degrees Celsius]
SOIL_TEMP_WEST_10CM             [degrees Celsius]
SOIL_TEMP_WEST_25CM             [degrees Celsius]
SOIL_TEMP_WEST_50CM             [degrees Celsius]
SOIL_TEMP_WEST_75CM             [degrees Celsius]
SOIL_TEMP_WEST_100CM            [degrees Celsius]
RAINFALL                        [millimeters]
DOWN_SOLAR_RAD_ABV_CNPY         [Watts][meter^-2]
UP_SOLAR_RAD_ABV_CNPY           [Watts][meter^-2]
NET_SOLAR_RAD_ABV_CNPY          [Watts][meter^-2]
DOWN_TOTAL_RAD_ABV_CNPY         [Watts][meter^-2]
UP_TOTAL_RAD_ABV_CNPY           [Watts][meter^-2]
AIR_TEMP_510CM                  [degrees Celsius]
AIR_TEMP_517CM                  [degrees Celsius]
AIR_TEMP_610CM                  [degrees Celsius]
AIR_TEMP_710CM                  [degrees Celsius]
AIR_TEMP_715CM                  [degrees Celsius]
AIR_TEMP_770CM                  [degrees Celsius]
AIR_TEMP_910CM                  [degrees Celsius]
WET_BULB_TEMP_510CM             [degrees Celsius]
WET_BULB_TEMP_517CM             [degrees Celsius]
WET_BULB_TEMP_610CM             [degrees Celsius]
WET_BULB_TEMP_710CM             [degrees Celsius]
WET_BULB_TEMP_715CM             [degrees Celsius]
WET_BULB_TEMP_770CM             [degrees Celsius]
WET_BULB_TEMP_910CM             [degrees Celsius]
WET_BULB_TEMP_ABV_CNPY          [degrees Celsius]
VAPOR_PRESS_510CM               [kiloPascals]
VAPOR_PRESS_517CM               [kiloPascals]
VAPOR_PRESS_610CM               [kiloPascals]
VAPOR_PRESS_710CM               [kiloPascals]
VAPOR_PRESS_715CM               [kiloPascals]
VAPOR_PRESS_770CM               [kiloPascals]
VAPOR_PRESS_910CM               [kiloPascals]
VAPOR_PRESS_ABV_CNPY            [kiloPascals]
SURF_PRESS                      [kiloPascals]
DOWN_LONGWAVE_RAD_ABV_CNPY      [Watts][meter^-2]
UP_LONGWAVE_RAD_ABV_CNPY        [Watts][meter^-2]
CORR_NET_RAD_ABV_CNPY           [Watts][meter^-2]
ALBEDO                          [unitless]
CNPY_AIR_TEMP_160CM             [degrees Celsius]
CNPY_WET_BULB_TEMP_160CM        [degrees Celsius]
CNPY_VAPOR_PRESS_160CM          [kiloPascals]
MEAN_SMALL_TREE_BIOMASS_TEMP    [degrees Celsius]
MEAN_MEDIUM_TREE_BIOMASS_TEMP   [degrees Celsius]
MEAN_LARGE_TREE_BIOMASS_TEMP    [degrees Celsius]
TOTAL_HEAT_STORAGE_NORTH        [Watts][meter^-2]
TOTAL_HEAT_STORAGE_WEST         [Watts][meter^-2]
MEAN_TOTAL_HEAT_STORAGE         [Watts][meter^-2]
BIO_HEAT_STORAGE_NORTH          [Watts][meter^-2]
BIO_HEAT_STORAGE_WEST           [Watts][meter^-2]
MEAN_BIO_HEAT_STORAGE           [Watts][meter^-2]
SENSIBLE_AIR_HEAT_STORAGE       [Watts][meter^-2]
```

```
LATENT_AIR_HEAT_STORAGE          [Watts][meter^-2]
SOIL_HEAT_STORAGE_NORTH_10CM     [Watts][meter^-2]
SOIL_HEAT_STORAGE_WEST_10CM      [Watts][meter^-2]
MEAN_SPECIFIC_HUM_ABV_CNPY       [grams][kilogram^-1]
SDEV_SPECIFIC_HUM_ABV_CNPY       [grams][kilogram^-1]
MEAN_W_WIND_SPEED_ABV_CNPY       [meters][second^-1]
SDEV_W_WIND_SPEED_ABV_CNPY       [meters][second^-1]
REL_HUM_ABV_CNPY                 [percent]
CRTFCN_CODE                      [none]
REVISION_DATE                    [DD-MON-YY]
```

The measurement units for the parameters contained in the porometry data files on the CD-ROM are:

```
         Column Name                              Units
------------------------------   -------------------------------------------------
SITE_NAME                        [none]
SUB_SITE                         [none]
DATE_OBS                         [DD-MON-YY]
TIME_OBS                         [HHMM GMT]
TREE_HT_CLASS                    [meters]
MEASUREMENT_HT_CLASS             [meters]
STOMATAL_CONDUCT_H2O             [millimeters H2O][second^-1]
CRTFCN_CODE                      [none]
REVISION_DATE                    [DD-MON-YY]
```

7.3.4 Data Source

The sources of the parameter values contained in the flux data files on the CD-ROM are:

```
         Column Name                           Data Source
------------------------------   -------------------------------------------------
SITE_NAME                        [Assigned by BORIS.]
SUB_SITE                         [Assigned by BORIS.]
DATE_OBS                         [Supplied by Investigator.]
TIME_OBS                         [Supplied by Investigator.]
SENSIBLE_HEAT_FLUX_ABV_CNPY      [sonic anemometer and thermocouple]
LATENT_HEAT_FLUX_ABV_CNPY        [sonic anemometer and krypton hygrometer]
NET_RAD_ABV_CNPY                 [net pyrradiometer]
CO2_FLUX_ABV_CNPY                [IRGA and sonic anemometer]
CO2_CONC_ABV_CNPY                [IRGA]]
CO2_STORAGE                      [IRGA and sonic anemometer]
CO2_FLUX_ABV_PLUS_STORAGE        [IRGA and sonic anemometer]
NIGHT_CO2_FLUX_ABV_CNPY          [Supplied by Investigator.]
DOWN_PPFD_ABV_CNPY               [quantum sensor]
UP_PPFD_ABV_CNPY                 [quantum sensor]
WIND_SPEED_510CM                 [anemometer]
WIND_SPEED_517CM                 [anemometer]
WIND_SPEED_610CM                 [anemometer]
WIND_SPEED_710CM                 [anemometer]
WIND_SPEED_715CM                 [anemometer]
WIND_SPEED_770CM                 [anemometer]
WIND_SPEED_910CM                 [anemometer]
WIND_SPEED_ABV_CNPY              [anemometer]
MEAN_WIND_DIR_MAG_ABV_CNPY       [wind vane]
SDEV_WIND_DIR_MAG_ABV_CNPY       [wind vane]
```

```
AIR_TEMP_ABV_CNPY                    [thermocouple]
H2O_FLUX_ABV_CNPY                    [sonic anemometer and krypton hygrometer]
SOIL_HEAT_FLUX_NORTH_10CM            [heat flux plate]
SOIL_HEAT_FLUX_WEST_10CM             [heat flux plate]
SOIL_TEMP_NORTH_1CM                  [thermocouple]
SOIL_TEMP_NORTH_5CM                  [thermocouple]
SOIL_TEMP_NORTH_10CM                 [thermocouple]
SOIL_TEMP_NORTH_25CM                 [thermocouple]
SOIL_TEMP_NORTH_50CM                 [thermocouple]
SOIL_TEMP_NORTH_75CM                 [thermocouple]
SOIL_TEMP_WEST_1CM                   [thermocouple]
SOIL_TEMP_WEST_5CM                   [thermocouple]
SOIL_TEMP_WEST_10CM                  [thermocouple]
SOIL_TEMP_WEST_25CM                  [thermocouple]
SOIL_TEMP_WEST_50CM                  [thermocouple]
SOIL_TEMP_WEST_75CM                  [thermocouple]
SOIL_TEMP_WEST_100CM                 [thermocouple]
RAINFALL                             [tipping bucket gauge]
DOWN_SOLAR_RAD_ABV_CNPY              [pyranometer]
UP_SOLAR_RAD_ABV_CNPY                [pyranometer]
NET_SOLAR_RAD_ABV_CNPY               [Supplied by Investigator.]
DOWN_TOTAL_RAD_ABV_CNPY              [Supplied by Investigator.]
UP_TOTAL_RAD_ABV_CNPY                [Supplied by Investigator.]
AIR_TEMP_510CM                       [thermocouple]
AIR_TEMP_517CM                       [thermocouple]
AIR_TEMP_610CM                       [thermocouple]
AIR_TEMP_710CM                       [thermocouple]
AIR_TEMP_715CM                       [thermocouple]
AIR_TEMP_770CM                       [thermocouple]
AIR_TEMP_910CM                       [thermocouple]
WET_BULB_TEMP_510CM                  [thermocouple]
WET_BULB_TEMP_517CM                  [thermocouple]
WET_BULB_TEMP_610CM                  [thermocouple]
WET_BULB_TEMP_710CM                  [thermocouple]
WET_BULB_TEMP_715CM                  [thermocouple]
WET_BULB_TEMP_770CM                  [thermocouple]
WET_BULB_TEMP_910CM                  [thermocouple]
WET_BULB_TEMP_ABV_CNPY               [thermocouple]
VAPOR_PRESS_510CM                    [temperature/relative humidity sensor]
VAPOR_PRESS_517CM                    [temperature/relative humidity sensor]
VAPOR_PRESS_610CM                    [temperature/relative humidity sensor]
VAPOR_PRESS_710CM                    [temperature/relative humidity sensor]
VAPOR_PRESS_715CM                    [temperature/relative humidity sensor]
VAPOR_PRESS_770CM                    [temperature/relative humidity sensor]
VAPOR_PRESS_910CM                    [temperature/relative humidity sensor]
VAPOR_PRESS_ABV_CNPY                 [temperature/relative humidity sensor]
SURF_PRESS                           [pressure sensor]
DOWN_LONGWAVE_RAD_ABV_CNPY           [pyrgeometer]
UP_LONGWAVE_RAD_ABV_CNPY             [pyrgeometer]
CORR_NET_RAD_ABV_CNPY                [Supplied by Investigator.]
ALBEDO                               [Supplied by Investigator.]
CNPY_AIR_TEMP_160CM                  [thermocouple]
CNPY_WET_BULB_TEMP_160CM             [thermocouple]
CNPY_VAPOR_PRESS_160CM               [temperature/relative humidity sensor]
```

```
MEAN_SMALL_TREE_BIOMASS_TEMP     [thermocouple]
MEAN_MEDIUM_TREE_BIOMASS_TEMP    [thermocouple]
MEAN_LARGE_TREE_BIOMASS_TEMP     [thermocouple]
TOTAL_HEAT_STORAGE_NORTH         [Supplied by Investigator.]
TOTAL_HEAT_STORAGE_WEST          [Supplied by Investigator.]
MEAN_TOTAL_HEAT_STORAGE          [Supplied by Investigator.]
BIO_HEAT_STORAGE_NORTH           [Supplied by Investigator.]
BIO_HEAT_STORAGE_WEST            [Supplied by Investigator.]
MEAN_BIO_HEAT_STORAGE            [Supplied by Investigator.]
SENSIBLE_AIR_HEAT_STORAGE        [Supplied by Investigator.]
LATENT_AIR_HEAT_STORAGE          [Supplied by Investigator.]
SOIL_HEAT_STORAGE_NORTH_10CM     [Supplied by Investigator.]
SOIL_HEAT_STORAGE_WEST_10CM      [Supplied by Investigator.]
MEAN_SPECIFIC_HUM_ABV_CNPY       [krypton hygrometer]
SDEV_SPECIFIC_HUM_ABV_CNPY       [krypton hygrometer]
MEAN_W_WIND_SPEED_ABV_CNPY       [sonic anemometer]
SDEV_W_WIND_SPEED_ABV_CNPY       [sonic anemometer]
REL_HUM_ABV_CNPY                 [temperature/relative humidity sensor]
CRTFCN_CODE                      [Assigned by BORIS.]
REVISION_DATE                    [Assigned by BORIS.]
```

The sources of the parameter values contained in the porometry data files on the CD-ROM are:

```
        Column Name                         Data Source
------------------------------   ------------------------------------------------
SITE_NAME                        [Assigned by BORIS.]
SUB_SITE                         [Assigned by BORIS.]
DATE_OBS                         [Supplied by Investigator.]
TIME_OBS                         [Supplied by Investigator.]
TREE_HT_CLASS                    [Supplied by Investigator.]
MEASUREMENT_HT_CLASS             [Supplied by Investigator.]
STOMATAL_CONDUCT_H2O             [Porometer]
CRTFCN_CODE                      [Assigned by BORIS.]
REVISION_DATE                    [Assigned by BORIS.]
```

7.3.5 Data Range

The following table gives information about the parameter values found in the flux data files on the CD-ROM.

Column Name	Minimum Data Value	Maximum Data Value	Missng Data Value	Unrel Data Value	Below Detect Limit	Data Not Cllctd
SITE_NAME	NSA-YJP-FLXTR	NSA-YJP-FLXTR	None	None	None	None
SUB_SITE	9TF10-FLX01	9TF10-FLX01	None	None	None	None
DATE_OBS	15-AUG-93	09-NOV-96	None	None	None	None
TIME_OBS	0	2330	None	None	None	None
SENSIBLE_HEAT_FLUX_ ABV_CNPY	-69.59	458.28	-999	None	None	None
LATENT_HEAT_FLUX_ABV _CNPY	-68.9	428.3	-999	None	None	None
NET_RAD_ABV_CNPY	-90.5	787	-999	None	None	None
CO2_FLUX_ABV_CNPY	-16.1	32.757	-999	None	None	Blank
CO2_CONC_ABV_CNPY	288.4	435.3	-999	None	None	Blank
CO2_STORAGE	-5.814	7.23	-999	None	None	Blank

CO2_FLUX_ABV_PLUS_ STORAGE	-16.09	10.494	-999	None	None	Blank
NIGHT_CO2_FLUX_ABV_ CNPY	-2.619	5.748	-999	None	None	Blank
DOWN_PPFD_ABV_CNPY	0	2100	-999	None	None	None
UP_PPFD_ABV_CNPY	0	360	-999	None	None	None
WIND_SPEED_510CM	.199	5.168	-999	None	None	Blank
WIND_SPEED_517CM	.199	6.223	-999	None	None	Blank
WIND_SPEED_610CM	.199	6.848	-999	None	None	Blank
WIND_SPEED_710CM	.199	6.022	-999	None	None	Blank
WIND_SPEED_715CM	.199	7.3	-999	None	None	Blank
WIND_SPEED_770CM	.199	7.59	-999	None	None	Blank
WIND_SPEED_910CM	.199	6.547	-999	None	None	Blank
WIND_SPEED_ABV_CNPY	.197	8.32	-999	None	None	None
MEAN_WIND_DIR_MAG_ ABV_CNPY	0	359.9	-999	None	None	None
SDEV_WIND_DIR_MAG_ ABV_CNPY	0	78.1	-999	None	None	None
AIR_TEMP_ABV_CNPY	-17.28	30.11	-999	None	None	None
H2O_FLUX_ABV_CNPY	-1.5283	7.8144	-999	None	None	None
SOIL_HEAT_FLUX_NORTH _10CM	-31.4	73	-999	None	None	None
SOIL_HEAT_FLUX_WEST_ 10CM	-45.2	93.1	-999	None	None	None
SOIL_TEMP_NORTH_1CM	-1.86	31.61	-999	None	None	None
SOIL_TEMP_NORTH_5CM	-.44	24.64	-999	None	None	None
SOIL_TEMP_NORTH_10CM	-.65	20.99	-999	None	None	None
SOIL_TEMP_NORTH_25CM	-.66	17.66	-999	None	None	Blank
SOIL_TEMP_NORTH_50CM	-.7	15.1	-999	None	None	Blank
SOIL_TEMP_NORTH_75CM	-.65	13.26	-999	None	None	Blank
SOIL_TEMP_WEST_1CM	-2.9	34.43	-999	None	None	None
SOIL_TEMP_WEST_5CM	-.08	24.65	-999	None	None	None
SOIL_TEMP_WEST_10CM	-.15	19.55	-999	None	None	None
SOIL_TEMP_WEST_25CM	-.13	16.19	-999	None	None	None
SOIL_TEMP_WEST_50CM	-.2	13.87	-999	None	None	None
SOIL_TEMP_WEST_75CM	-.3	12.2	-999	None	None	None
SOIL_TEMP_WEST_100CM	-.24	10.89	-999	None	None	None
RAINFALL	0	6.35	-999	None	None	None
DOWN_SOLAR_RAD_ABV_ CNPY	0	1021	-999	None	None	None
UP_SOLAR_RAD_ABV_ CNPY	0	188.2	-999	None	None	None
NET_SOLAR_RAD_ABV_ CNPY	0	891.4	-999	None	None	None
DOWN_TOTAL_RAD_ABV_ CNPY	179.45	1365.5	-999	None	None	None
UP_TOTAL_RAD_ABV_ CNPY	229.8	632.9	-999	None	None	None
AIR_TEMP_510CM	.373	26.8	-999	None	None	Blank
AIR_TEMP_517CM	-17.43	30.4	-999	None	None	Blank
AIR_TEMP_610CM	-.013	30.18	-999	None	None	Blank
AIR_TEMP_710CM	2.581	26.57	-999	None	None	Blank
AIR_TEMP_715CM	.156	29.45	-999	None	None	Blank
AIR_TEMP_770CM	-17.36	30.14	-999	None	None	Blank

AIR_TEMP_910CM	3.752	26.37	-999	None	None	Blank
WET_BULB_TEMP_510CM	.11	18.95	-999	None	None	Blank
WET_BULB_TEMP_517CM	-.136	19	-999	None	None	Blank
WET_BULB_TEMP_610CM	-.043	18.95	-999	None	None	Blank
WET_BULB_TEMP_710CM	3.641	18.78	-999	None	None	Blank
WET_BULB_TEMP_715CM	.077	18.95	-999	None	None	Blank
WET_BULB_TEMP_770CM	.132	18.94	-999	None	None	Blank
WET_BULB_TEMP_910CM	2.959	18.77	-999	None	None	Blank
WET_BULB_TEMP_ABV_CNPY	.156	18.92	-999	None	None	Blank
VAPOR_PRESS_510CM	.5983	1.9357	-999	None	None	Blank
VAPOR_PRESS_517CM	.4654	1.9731	-999	None	None	Blank
VAPOR_PRESS_610CM	.4854	1.9724	-999	None	None	Blank
VAPOR_PRESS_710CM	.5872	1.9041	-999	None	None	Blank
VAPOR_PRESS_715CM	.4602	1.9717	-999	None	None	Blank
VAPOR_PRESS_770CM	.4592	1.9731	-999	None	None	Blank
VAPOR_PRESS_910CM	.6067	1.9161	-999	None	None	Blank
VAPOR_PRESS_ABV_CNPY	.1338	2.3719	-999	None	None	None
SURF_PRESS	95.8	99.6	-999	None	None	Blank
DOWN_LONGWAVE_RAD_ABV_CNPY	155.5	421.12	-999	None	None	None
UP_LONGWAVE_RAD_ABV_CNPY	229.8	524.7	-999	None	None	None
CORR_NET_RAD_ABV_CNPY	-95.01	788.3	-999	None	None	Blank
ALBEDO	0	.965	-999	None	None	None
CNPY_AIR_TEMP_160CM	-4.114	31.87	-999	None	None	Blank
CNPY_WET_BULB_TEMP_160CM	-4.17	19.32	-999	None	None	Blank
CNPY_VAPOR_PRESS_160CM	.4415	2.0113	-999	None	None	Blank
MEAN_SMALL_TREE_BIOMASS_TEMP	-24.48	39.03	-999	None	None	None
MEAN_MEDIUM_TREE_BIOMASS_TEMP	-23.89	37	-999	None	None	None
MEAN_LARGE_TREE_BIOMASS_TEMP	-21.88	35.56	-999	None	None	None
TOTAL_HEAT_STORAGE_NORTH	-146.1	102.7	-999	None	None	Blank
TOTAL_HEAT_STORAGE_WEST	-74.3	148.3	-999	None	None	Blank
MEAN_TOTAL_HEAT_STORAGE	-62.1	89.2	-999	None	None	Blank
BIO_HEAT_STORAGE_NORTH	-12	9.2	-999	None	None	Blank
BIO_HEAT_STORAGE_WEST	-25.3	15	-999	None	None	Blank
MEAN_BIO_HEAT_STORAGE	-10.5	6.2	-999	None	None	Blank
SENSIBLE_AIR_HEAT_STORAGE	-44	22.6	-999	None	None	None
LATENT_AIR_HEAT_STORAGE	-34.3	52.3	-999	None	None	None
SOIL_HEAT_STORAGE_	-66.7	46.8	-999	None	None	Blank

```
NORTH_10CM
SOIL_HEAT_STORAGE_      -89.8           76              -999    None    None    Blank
WEST_10CM
MEAN_SPECIFIC_HUM_      2.41            22.56           -999    None    None    Blank
ABV_CNPY
SDEV_SPECIFIC_HUM_      .012            10.84           -999    None    None    Blank
ABV_CNPY
MEAN_W_WIND_SPEED_      -1.997          1.979           -999    None    None    Blank
ABV_CNPY
SDEV_W_WIND_SPEED_      0               4.424           -999    None    None    Blank
ABV_CNPY
REL_HUM_ABV_CNPY        12.5            125.7           -999    None    None    Blank
CRTFCN_CODE             CPI             CPI             None    None    None    None
REVISION_DATE           15-JAN-99       20-JAN-99       None    None    None    None
------------------------------------------------------------------------------------
```

The following table gives information about the parameter values found in the porometry data files on the CD-ROM.

```
                        Minimum         Maximum         Missng  Unrel   Below   Data
                        Data            Data            Data    Data    Detect  Not
Column Name             Value           Value           Value   Value   Limit   Cllctd
------------------------------------------------------------------------------------
SITE_NAME               NSA-YJP-FLXTR   NSA-YJP-FLXTR   None    None    None    None
SUB_SITE                9TF10-PR996     9TF10-PRWET     None    None    None    None
DATE_OBS                05-JUN-94       07-OCT-96       None    None    None    None
TIME_OBS                330             2330            None    None    None    None
TREE_HT_CLASS           <1.3            >1.3            None    None    None    None
MEASUREMENT_HT_CLASS    <1.3            >1.3            None    None    None    None
STOMATAL_CONDUCT_H2O    .0162           14.3745         -999    None    None    None
CRTFCN_CODE             CPI             CPI             None    None    None    None
REVISION_DATE           03-FEB-99       03-FEB-99       None    None    None    None
------------------------------------------------------------------------------------
Minimum Data Value  -- The minimum value found in the column.
Maximum Data Value  -- The maximum value found in the column.
Missng Data Value   -- The value that indicates missing data. This is used to
                       indicate that an attempt was made to determine the
                       parameter value, but the attempt was unsuccessful.
Unrel Data Value    -- The value that indicates unreliable data.  This is used
                       to indicate an attempt was made to determine the
                       parameter value, but the value was deemed to be
                       unreliable by the analysis personnel.
Below Detect Limit  -- The value that indicates parameter values below the
                       instruments detection limits.  This is used to
                       indicate that an attempt was made to determine the
                       parameter value, but the analysis personnel determined
                       that the parameter value was below the detection
                       limit of the instrumentation.
Data Not Cllctd     -- This value indicates that no attempt was made to
                       determine the parameter value.  This usually
                       indicates that BORIS combined several similar but
                       not identical data sets into the same data base table
                       but this particular science team did not
                       measure that parameter.
```

```
Blank -- Indicates that blank spaces are used to denote that type of value.
N/A   -- Indicates that the value is not applicable to the respective column.
None  -- Indicates that no values of that sort were found in the column.
    ------------------------------------------------------------------------
```

7.4 Sample Data Record
   The following are wrapped versions of flux data records from a sample data file on the CD-ROM.

```
SITE_NAME,SUB_SITE,DATE_OBS,TIME_OBS,SENSIBLE_HEAT_FLUX_ABV_CNPY,
LATENT_HEAT_FLUX_ABV_CNPY,NET_RAD_ABV_CNPY,CO2_FLUX_ABV_CNPY,CO2_CONC_ABV_CNPY,
CO2_STORAGE,CO2_FLUX_ABV_PLUS_STORAGE,NIGHT_CO2_FLUX_ABV_CNPY,DOWN_PPFD_ABV_CNPY,
UP_PPFD_ABV_CNPY,WIND_SPEED_510CM,WIND_SPEED_517CM,WIND_SPEED_610CM,
WIND_SPEED_710CM,WIND_SPEED_715CM,WIND_SPEED_770CM,WIND_SPEED_910CM,
WIND_SPEED_ABV_CNPY,MEAN_WIND_DIR_MAG_ABV_CNPY,SDEV_WIND_DIR_MAG_ABV_CNPY,
AIR_TEMP_ABV_CNPY,H2O_FLUX_ABV_CNPY,SOIL_HEAT_FLUX_NORTH_10CM,
SOIL_HEAT_FLUX_WEST_10CM,SOIL_TEMP_NORTH_1CM,SOIL_TEMP_NORTH_5CM,
SOIL_TEMP_NORTH_10CM,SOIL_TEMP_NORTH_25CM,SOIL_TEMP_NORTH_50CM,
SOIL_TEMP_NORTH_75CM,SOIL_TEMP_WEST_1CM,SOIL_TEMP_WEST_5CM,SOIL_TEMP_WEST_10CM,
SOIL_TEMP_WEST_25CM,SOIL_TEMP_WEST_50CM,SOIL_TEMP_WEST_75CM,
SOIL_TEMP_WEST_100CM,RAINFALL,DOWN_SOLAR_RAD_ABV_CNPY,UP_SOLAR_RAD_ABV_CNPY,
NET_SOLAR_RAD_ABV_CNPY,DOWN_TOTAL_RAD_ABV_CNPY,UP_TOTAL_RAD_ABV_CNPY,
AIR_TEMP_510CM,AIR_TEMP_517CM,AIR_TEMP_610CM,AIR_TEMP_710CM,AIR_TEMP_715CM,
AIR_TEMP_770CM,AIR_TEMP_910CM,WET_BULB_TEMP_510CM,WET_BULB_TEMP_517CM,
WET_BULB_TEMP_610CM,WET_BULB_TEMP_710CM,WET_BULB_TEMP_715CM,WET_BULB_TEMP_770CM,
WET_BULB_TEMP_910CM,WET_BULB_TEMP_ABV_CNPY,VAPOR_PRESS_510CM,VAPOR_PRESS_517CM,
VAPOR_PRESS_610CM,VAPOR_PRESS_710CM,VAPOR_PRESS_715CM,VAPOR_PRESS_770CM,
VAPOR_PRESS_910CM,VAPOR_PRESS_ABV_CNPY,SURF_PRESS,DOWN_LONGWAVE_RAD_ABV_CNPY,
UP_LONGWAVE_RAD_ABV_CNPY,CORR_NET_RAD_ABV_CNPY,ALBEDO,CNPY_AIR_TEMP_160CM,
CNPY_WET_BULB_TEMP_160CM,CNPY_VAPOR_PRESS_160CM,MEAN_SMALL_TREE_BIOMASS_TEMP,
MEAN_MEDIUM_TREE_BIOMASS_TEMP,MEAN_LARGE_TREE_BIOMASS_TEMP,
TOTAL_HEAT_STORAGE_NORTH,TOTAL_HEAT_STORAGE_WEST,MEAN_TOTAL_HEAT_STORAGE,
BIO_HEAT_STORAGE_NORTH,BIO_HEAT_STORAGE_WEST,MEAN_BIO_HEAT_STORAGE,
SENSIBLE_AIR_HEAT_STORAGE,LATENT_AIR_HEAT_STORAGE,SOIL_HEAT_STORAGE_NORTH_10CM,
SOIL_HEAT_STORAGE_WEST_10CM,MEAN_SPECIFIC_HUM_ABV_CNPY,
SDEV_SPECIFIC_HUM_ABV_CNPY,MEAN_W_WIND_SPEED_ABV_CNPY,SDEV_W_WIND_SPEED_ABV_CNPY,
REL_HUM_ABV_CNPY,CRTFCN_CODE,REVISION_DATE
'NSA-YJP-FLXTR','9TF10-FLX01',24-MAY-94,630,-999.0,-999.0,-63.08,-999.0,-999.0,
-999.0,-999.0,-999.0,0.0,0.0,,1.358,1.658,,1.869,1.976,,2.266,273.7,5.462,8.64,
-999.0,1.1,-3.4,4.346,5.635,6.001,-999.0,-999.0,-999.0,3.906,5.162,5.327,4.298,
2.119,.784,.178,0.0,0.0,0.0,0.0,-999.0,-999.0,,7.03,7.61,,7.98,8.17,,,,5.496,
-999.0,,5.926,-999.0,,6.332,,.8022,-999.0,,.7953,-999.0,,.8051,,-999.0,-999.0,
-62.71,0.0,3.51,3.15,.7423,.05,1.225,5.068,-14.7,-20.5,,-.7,-1.6,,-3.5,-.8,-10.8,
-11.2,-999.0,-999.0,-999.0,-999.0,,'CPI',15-JAN-99
'NSA-YJP-FLXTR','9TF10-FLX01',24-MAY-94,700,-999.0,-999.0,-59.15,-999.0,-999.0,
-999.0,-999.0,-999.0,0.0,0.0,,1.366,1.623,,1.837,1.95,,2.356,273.0,2.121,7.83,
-999.0,-.1,-5.5,3.809,5.312,5.824,-999.0,-999.0,-999.0,3.354,4.826,5.144,4.274,
2.154,.803,.188,0.0,0.0,0.0,0.0,-999.0,-999.0,,6.054,6.557,,6.92,7.14,,,,4.949,
-999.0,,5.387,-999.0,,5.962,,.7966,-999.0,,.7955,-999.0,,.8099,,-999.0,-999.0,
-58.08,0.0,3.276,2.959,.7348,-.84,.418,4.349,-15.4,-20.3,,-.5,-1.0,,-3.3,-.8,
-10.7,-9.7,-999.0,-999.0,-999.0,-999.0,,'CPI',15-JAN-99
```

The following are wrapped versions of porometry data records from a sample data file on the CD-ROM.

```
SITE_NAME,SUB_SITE,DATE_OBS,TIME_OBS,TREE_HT_CLASS,MEASUREMENT_HT_CLASS,
STOMATAL_CONDUCT_H2O,CRTFCN_CODE,REVISION_DATE
'NSA-YJP-FLXTR','9TF10-PR996',16-SEP-96,1730,'>1.3','>1.3',2.199,'CPI',03-FEB-99
'NSA-YJP-FLXTR','9TF10-PR996',16-SEP-96,1730,'<1.3','<1.3',1.042,'CPI',03-FEB-99
```

8. Data Organization

8.1 Data Granularity
The smallest unit of data tracked by BORIS was data collected at a given site on a given date.

8.2 Data Format
The Compact Disk-Read-Only Memory (CD-ROM) files contain American Standard Code for Information Interchange (ASCII) numerical and character fields of varying length separated by commas. The character fields are enclosed with single apostrophe marks. There are no spaces between the fields.

Each data file on the CD-ROM has four header lines of Hyper-Text Markup Language (HTML) code at the top. When viewed with a Web browser, this code displays header information (data set title, location, date, acknowledgments, etc.) and a series of HTML links to associated data files and related data sets. Line 5 of each data file is a list of the column names, and line 6 and following lines contain the actual data.

9. Data Manipulations

9.1 Formulae

Net Solar Radiation (W/m²)
Net solar radiation (K*) is the difference between incoming solar radiation (Kd) and reflected solar radiation (Ku):

$$K* = Kd - Ku \qquad (9.1)$$

Incoming Longwave Radiation (W/m²)
Incoming longwave radiation (Ld) is calculated as a residual from the net radiation balance, where net radiation (Q*) is the sum of net solar radiation (K*, see e.g. 9.1) and net longwave radiation (L*). L* is the difference between incoming longwave radiation (Ld) and outgoing longwave radiation (Lu).

$$Q* = Kd - Ku + Ld - Lu \qquad (9.2)$$

Total Incoming Radiation (W/m²)
Total incoming radiation (Qd) is the sum of all incoming radiation:

$$Qd = Kd + Ld \qquad (9.3)$$

Total Outgoing Radiation (W/m²)
Total outgoing radiation (Qu) is the sum of all outgoing radiation:

$$Qu = Ku + Lu \qquad (9.4)$$

Net Radiation corrected (W/m²)

Measured net radiation (Q*) was corrected using a set of site-specific day- and night-time equations developed by Hodges and Smith (1997). These equations (shown below) were used for all years of data, excluding data collected in 1993 at both fen and YJP. The use of the day or night equation is based on measured incoming solar radiation. When Kd>5.00 W/m², daytime equations are used. The relevant equations for the fen and YJP are:

```
Site           Time of day        Correction equation
Fen              DAY               Q*corr = 0.957(Q*) + 3.2           (9.5)
                 NIGHT             Q*corr = 1.079(Q*) + 11.1          (9.6)
YJP              DAY               Q*corr = 0.992(Q*) + 7.6           (9.7)
                 NIGHT             Q*corr = 1.178(Q*) + 11.6          (9.8)
```

Surface Albedo (dimensionless)

Surface albedo (a) is the ratio of the amount of radiation reflected by a body to the amount incident upon it:

$$a = Ku/Kd \qquad (9.9)$$

Total CO$_2$ Flux (umol/m²/s)

The total CO$_2$ flux (FCO$_2$) is the sum of the eddy flux (Fe$_{CO2}$) and the storage flux (Fs$_{CO2}$):

$$F_{CO2} = Fe_{CO2} + Fs_{CO2} \qquad (9.10)$$

In 1994 and 1996 at the YJP site, a night model (CO$_2$night) was used in the calculation of the total CO$_2$ flux (when Kd=0), and

$$CO_2night = -2.4883 + 0.82337(Ts10avg) - 0.6777(Ts75avg) \qquad (9.11)$$

where Ts10avg and Ts75avg are the average soil temperatures from the north and west zones from a depth of 10 and 75 cm, respectively. Then,

$$F_{CO2} = CO_2night + Fs_{CO2} \qquad (9.12)$$

Heat Storage (W/m²)

Total heat storage (G_total) is based on the sum of heat storage from several environmental compartments:

$$G\_total = G + Ga + Ge + Gveg \qquad (9.13)$$

where: G = soil heat flux
Ga = sensible heat storage in the air
Ge = latent heat storage in the air
Gveg = heat storage in the vegetation

Only G is measured, and the remaining variables are calculated using the formulae given by Thom (1975):

$$Ga(T) = 0.33 \ zr \ dTa(t) \qquad (9.14)$$
$$Ge(T) = 0.5 \ zr \ de(t) \qquad (9.15)$$
$$Gveg(T) = 0.8 \ Mv \ dTb(t) \qquad (9.16)$$

where zr is the reference height (in this case the height of the net pyrradiometer)(m); dTa, de, and dTb are the rates of change in air temperature (°C/s), vapor pressure (kPa/s), and biomass temperature (°C/s), respectively, for time step t; and Mv is the standing green mass of vegetation over unit area (kg/m^2). Theoretically, Ga and Ge are integrated over the height interval between the surface and zr. In this study, the calculations were performed for discrete layers represented by the profile psychrometer heights and summed to get the totals. The calculation of all minor heat storage terms in the energy balance were calculated with the Fortran program called STORAG. An explanation of this program is given in Section 9.1.1, and a description of the command files used to process the data is given in Section 9.2.1.

Ground heat flux at the YJP site is computed in the usual sense, where the heat flux plate reading is summed with heat storage from the soil layer between the plate and soil surface.

The operational equations are:

$$G = G(z) + S \qquad\qquad (9.17)$$
$$S = CdTs(t) \, z/1800 \qquad (9.18)$$
$$C = Cm \, Xm + Cw \, Xw + Co \, Xo \quad (9.19)$$

where G is the ground heat flux at the soil surface integrated over a 30-minute time interval (W/m^2), G(z) is the soil heat flux measured at depth z (W/m^2), and S is the flux equivalent to the heat stored between the surface and the heat flux plates during the time interval (t=1800s) (W/m^2). C is the volumetric heat capacity of the soil (J/m^3/°C), dTs(t) is the temperature change in the soil layer above the heat flux plate over the time interval (°C/s), and z is the depth of the heat flux plates (m). The volumetric heat capacity is obtained from measurements of the volume fractions (X) of the mineral, water, and organic soil components (subscript m, w, and o, respectively) and their respective heat capacities (Cm, Cw, and Co).

Heat storage calculated for the YJP site was distinguished by zone in 1994 and 1996. Separate soil heat fluxes were measured for the north and west zones (G(z)n and G(z)w, respectively). Calculated variables include sensible heat storage in the air (Ga), latent heat storage in the air (Ge), and heat storage in the vegetation at both the north and west sites (Gvegn and Gvegw, respectively). Heat storage in the soil volume above 10 cm depth (G10) is also a part of G_total in 1994 and 1996, resulting in the following equations:

$$G\_totaln = G(z)n + Ga + Ge + Gvegn + G10 \qquad (9.20)$$
$$G\_totalw = G(z)w + Ga + Ge + Gvegw + G10 \qquad (9.21)$$

In 1993, an average value of the north and west zones is presented for G_total and Gveg.

Ground heat flux at the fen in 1994 only (Gfen) was computed by adjusting the heat flux plate readings from the hollow (Ghol) with a correction factor determined from calorimetric methods. In the following explanation, Gpla is equal to Ghol. Hence,

$$G = G(z)CF \qquad (9.22)$$
$$\text{where } CF = Gcal/Gpla \qquad (9.23)$$

in which CF is a correction factor (3.04) determined from calorimetric calculations of heat storage in the soil profile (Gcal) and the time-integrated flux measured by the heat flux plates (Gpla). Gpla is calculated by summing the 30-minute average heat flux plate readings multiplied by 1800 seconds over a specified time interval (usually 10-14 days). Gcal is the total heat storage in the soil profile calculated from individual soil layers represented by the measured temperature profile(s), plus the heat flux out the bottom of the soil profile (GB).

Heat storage in the individual layers, S(i) is computed as:

$$S(i) = CdT(t)z \qquad (9.24)$$

where symbols are defined as above. C varies between 3.48 x 10^6 J/m^3/°C for saturated peat soil and 0.58 x 10^6 J/m^3/°C for dry peat soil. The flux out the base of the soil profile is calculated as:

$$GB = -Ks \, dT/dz \qquad (9.25)$$

where -Ks is the thermal conductivity of saturated peat soil (0.5 W/m/°C) and dT/dz is the temperature gradient at the base of the soil profile.

In 1993, 1995, and 1996, no correction factor was applied to the fen's soil heat flux data (see Section 10.2.2). In these years, the soil heat flux from the hollow (Ghol) was used in the calculations of G_total.

Stem Temperatures (°C)

Stem temperatures were recorded at YJP in 1993, 1994, and 1996 from both the north and west sites at YJP. Stem temperatures from small (Tbsw), medium (Tbmw), and large trees (Tblw) were recorded at the west site, whereas only small trees were sampled at the north site (Tbsn). Stem temperatures recorded in the data files were taken from the west site, with the exception of stem temperatures from small trees. Tbs is an average of the stem temperatures from both the north and west sites:

$$Tbs = (Tbsn + Tbsw)/2 \qquad (9.26)$$

Specific Humidity (g/kg)

Specific humidity (SH) and the standard deviation of specific humidity (sSH) were calculated using measured air temperature (T_air), vapor density (q), and the standard deviation of ln q (sln q).

Air density (rho) is found as a function of T_air, where:

```
if     T_air>30   then rho = 1.149 - 0.0036 (T_air - 30.01)   (9.27)
if  25>T_air>30   then rho = 1.168 - 0.0038 (T_air - 25.01)   (9.28)
if  20>T_air>25   then rho = 1.188 - 0.0040 (T_air - 20.01)   (9.29)
if  15>T_air>20   then rho = 1.209 - 0.0042 (T_air - 15.01)   (9.30)
if  10>T_air>15   then rho = 1.230 - 0.0042 (T_air - 10.01)   (9.31)
if   5>T_air>10   then rho = 1.252 - 0.0044 (T_air -  5.01)   (9.32)
if   0>T_air>5    then rho = 1.275 - 0.0046 (T_air -  0.01)   (9.33)
if  -5>T_air>0    then rho = 1.229 - 0.0048 (T_air +  4.99)   (9.34)
if -10>T_air>-5   then rho = 1.324 - 0.0050 (T_air +  9.99)   (9.35)
if -15>T_air>-10  then rho = 1.350 - 0.0050 (T_air + 14.99)   (9.36)
if -20>T_air>-15  then rho = 1.376 - 0.0054 (T_air + 19.99)   (9.37)
```

The specific humidity is found from the vapor density (g/m^3), measured by the krypton hygrometer at each site, and

$$q = (\ln s - \ln v)/kx \qquad (9.38)$$

where s = the signal voltage from the hygrometer (mv), v is the intercept of the hygrometer's calibration (4054 mv for the fen and 4528 mv for the YJP), k is absorption coefficient for water vapor (-0.141 m^3/g/cm for the fen and -0.133 m^3/g/cm for the YJP), and x is the path length of the hygrometer (1.542 cm for the fen and 1.400 cm for the YJP). Then,

$$SH = q/rho \qquad (9.39) \text{ and}$$
$$sSH = (e^{|s\ln q|})/rho \qquad (9.40)$$

where s indicates the standard deviation.

Convective Heat Fluxes (H and LE)

The sensible heat flux was found from equation 3.2 which states that

$$H = rho\ Cp\ <w'T'> \qquad (9.41)$$

where the variables have their usual meanings. Webb (1982) showed that the air density and specific heat of air are functions of both the air's temperature and vapor pressure, and that air temperature had the largest control. Thus, in our calculations, the rho Cp term was corrected for changing temperature and air pressure as follows:

$$rho\ Cp = Cp(d)\ (P\ M/R\ T) \qquad (9.42)$$

where $Cp(d)$ is the specific heat of dry air, P is the atmospheric pressure, M is the molecular weight of dry air, R is the universal gas constant, and T is the air temperature. In the 1994 experiments, P was obtained from Thompson airport and read into the data logger once a day, usually about 1500 UTC, when the site was first visited. In 1996, analog pressure sensors at the YJP and fen were recorded P every half-hour. The air temperature that was used was the average value from the previous half-hour, which was updated on a continuous basis automatically by the data logger. The precision of this correction was improved in 1996 because we incorporated air pressure sensors into the measurement packages at each site, and this allowed the use of the previous half-hour's air pressure as well as temperature in equation 9.41.

The value of L, the latent heat of vaporization, in the eddy covariance measurement of latent heat flux (equation 3.1) was found as a function of air temperature from the equation

$$L = 2501 + (-2.363)\ T + (-0.00023)\ T^2 \qquad (9.43)$$

where T is the air temperature averaged over the previous half-hour. Equation 9.42 was part of the online calculations.

The krypton lamp in the hygrometer has two emission lines, a major line at 123.58 nm, and a minor line at 116.49 nm. Both lines are absorbed by both water vapor and oxygen. It is necessary to account for the effect of absorption by oxygen on the value of vapor density in order to correct the latent heat flux. The oxygen correction is a function of atmospheric pressure and temperature, and Tanner, et al. (1993) provide the appropriate equations to find the oxygen correction. At standard atmospheric pressure (101.3 kP) and temperature (305 K), the pressure correction is small in comparison to that caused by temperature, and it is usual to correct for oxygen absorption based only on temperature. This procedure was followed in this experiment.

Webb et al. (1980) described the influence of sensible heat and vapor fluxes that cause changes in the density of atmospheric constituents, and the necessary corrections to the flux associated with these fluctuations. These corrections are usually termed the Webb, Pearman, and Leuning (WPL) corrections, and they were applied to the latent heat flux in this experiment (Joiner, 1994). The WPL correction due to the sensible heat flux is approximately five times larger than that due to the vapor flux itself (Tanner et al., 1993).

Carbon Dioxide Flux

Because we used a closed-path IRGA and the air sample was delivered to the instrument through a sample tube, there is a time delay, or lag, in the concentration of CO_2, measured in the IRGA, and the measured vertical wind in the free atmosphere around the sonic. If the CO_2 concentration data were not corrected for lag, we would not calculate the correct covariance, and the flux of CO_2 would be incorrect. We found the lag for our CO_2 systems at fen and YJP empirically. While continuously monitoring the output of CO_2 and vertical wind, we introduced a bubble of nitrogen in the vicinity of the sample tube intake. The arrival of the nitrogen in the sample cell of the IRGA caused a discernable spike in the CO_2 time series. We identified formally the time of occurrence of the spike by lag correlation analysis of CO_2 concentration and vertical wind. The lag was where the correlation

coefficient between CO_2 and vertical wind was a maximum. Site-specific lag times were programmed into the data loggers at each site, and these lags allowed us to compute a covariance using the correct values of CO_2 and vertical wind.

The concentration of CO_2 measured by an IRGA is dependent on pressure. Changing pressure changes the calibration of the instrument (span/voltage difference) by changing the span. The span is the difference in concentration between the high and low span gases; in our case approximately 30 to 40 ppmv. The effect of changing pressure on the IRGA's calibration was corrected online.

Changes in the air's temperature and water vapor density, which in turn are related to the sensible and latent heat fluxes, affect the concentration of CO_2 and hence the flux of CO_2 (Webb et al., 1980). In postprocessing, the CO_2 flux was corrected for changing density and vapor flux (Joiner, 1994). The correction includes a correction for the cross-sensitivity of the IRGA to water vapor and carbon dioxide (Leuning and Moncrieff, 1990; Leuning and King, 1992).

9.1.1 Derivation Techniques and Algorithms

STORAG is the general name for a Fortran program that calculates the minor heat storage terms in the energy balance. There are several operational versions of the program that differ depending upon the available data (see Section 9.2.1). Also, ENBAL, a Fortran program to solve for the terms of the radiation balance, was used in the analysis. Both STORAG and ENBAL work on the principle of GET commands that read input data into memory from various files, and when sufficient variables are read to solve the control equations, the calculations get done and are stored in output tables that can be delivered to spreadsheets or plotting packages for further processing and plotting. There is a worked example of the operation of STORAG in Section 9.2.1 that illustrates not only the specific features of STORAG but also the general nature of both programs.

9.2 Data Processing Sequence

9.2.1 Processing Steps

Two versions of STORAG were used in the calculations of heat storage depending on what data were available: STORY94.exe and STORY96.exe. STORY94.exe, used on 1993, 1994, and 1995 data, calculated heat storage variables from wet-bulb and dry-bulb temperatures, net radiation, soil heat flux, and soil temperatures. STORY96.exe was used on the 1996 data where relative humidity (RH) was an input measured variable, which replaced its calculation using wet-bulb temperatures.

A command file is used to run the STORAG program. It comprises a list of GET statements that will select variables from a specified column in a specified file. The last two numbers in the GET statement are the slope and intercept of the equation to be used with that data. This is useful if the input data are in the wrong units and a linear calibration can be applied. Other variables are set using SET statements. Variables used in the STORY94 program are:

```
Q*       Net radiation
QGZ      Soil heat flux
TS1-3    Soil temperatures from depths of 1, 5, and 10 cm, respectively
TB       Biomass temperature (see Section 9.2.2)
TD1-6    Dry-bulb temperatures
Tw1-6    Wet-bulb temperatures (in STORY96 RH is used instead)
XW       Soil moisture content
HCS      Heat capacity of soil
TOL      Thickness of the organic layer
DS       Depth of temperature measurements
ZR       Height of the net radiation measurement
ZCQ      Height of canopy, height of net pyrradiometer
MV       Green mass of vegetation
CON      Constant used in equations determining Ga, Ge, and Gveg
```

An example of the command file used to run STORAG is listed in Table 16 for one day of data. All commands must be in capital letters, Q* and QGZ data must be 30-minute averages, and the remaining temperatures are 15-minute averages.

Table 16. Example command file for STORAG, a program to find the minor heat storage terms in the surface energy balance.

```
SETPAUSE OFF
CLEAR
TITLE   YJP NORTH FOREST SITE   ENERGY STORAGE   MAY-24-1994 (144)
SETTIME 0.25 0.25 95
GET(Q*)   Y94307E.144  (24X,F8.0)   1.0 0.0
GET(QGZ)  Y94307E.144  (112X,F8.0)  1.0 0.0
GET(TS1)  Y94157E.144  (200X,F8.0)  1.0 0.0
GET(TS2)  Y94157E.144  (208X,F8.0)  1.0 0.0
GET(TS3)  Y94157E.144  (216X,F8.0)  1.0 0.0
GET(TB)   Y94157E.144  (40X,F8.0)   1.0 0.0
GET(TD1)  Y94157E.144  (48X,F8.0)   1.0 0.0
GET(TD2)  Y94157E.144  (56X,F8.0)   1.0 0.0
GET(TD3)  Y94157E.144  (64X,F8.0)   1.0 0.0
GET(TD4)  Y94157E.144  (72X,F8.0)   1.0 0.0
GET(TD5)  Y94157E.144  (80X,F8.0)   1.0 0.0
GET(TD6)  Y94157E.144  (88X,F8.0)   1.0 0.0
GET(TW1)  Y94157E.144  (96X,F8.0)   1.0 0.0
GET(TW2)  Y94157E.144  (104X,F8.0)  1.0 0.0
GET(TW3)  Y94157E.144  (104X,F8.0)  1.0 0.0
GET(TW4)  Y94157E.144  (120X,F8.0)  1.0 0.0
GET(TW5)  Y94157E.144  (128X,F8.0)  1.0 0.0
GET(TW6)  Y94157E.144  (136X,F8.0)  1.0 0.0
SET(XW)   0.08 0.08
SET(HCS)  0.1455 0.2067
SET(TOL)  0.03
SET(DS)   0.01 0.05 0.1
SET(ZR)   1.5 5.07 6.0 7.05 7.6 10.2
SET(ZCQ)  3.0 11.60
SET(MV)   0.888
SET(CON)  0.8
SHOW
WRITE     Y94STORN.144
WRITESTO  Y94QSN.144
```

9.2.2 Processing Changes

Where one level of air temperature was missing from a file used in STORAG, the GET statement was changed to read the value from the nearest level. For example, if the third level of temperature is missing, the value from the fourth level could be used instead.

Mass of vegetation (MV) is zero in the fen calculations. For heat storage calculations at YJP in the west site, MV = 2.22. Because there were only small trees in the north site, MV = 0.888 for that site. Biomass temperature (TB) is zero in the fen calculations, whereas it is based on the stem temperatures at YJP. In the north site, TB = Tbsn. In the west site, the following weighted average, based on the percentage occurrence of small, medium, and large trees, was used to determine TB:

$$TB = 0.4 \, Tbsw + 0.486 \, Tbmw + 0.114 \, Tblw \qquad (9.44)$$

The STORAG program does not accept zero in the command file; therefore, the TB multiplier, the thickness of the organic layer (TOL), the height of the canopy, and the mass of vegetation (MV) were set to 0.000001 in the fen calculations, creating insignificant values in the calculated heat storage.

9.3 Calculations

9.3.1 Special Corrections/Adjustments

The following rules were followed in preparing the data files:

- Any small negative values of Kd and Ku (<1 W/m^2) were changed to zero and Ld, Qd, Qu, and the albedo were recalculated accordingly; negative values occur as a result of zero depression on the instruments.
- All negative values of incoming and reflected photosynthetic photon flux density (PPFDd and PPFDu) were changed to zero; as is the case with pyranometers, small negative values result from zero depression.
- When $FsCO_2$ was missing and Kd>0, then $F_{CO2} = Fe_{CO2}$
- When $FsCO_2$ was missing and Kd=0, then $F_{CO2} = CO_2night$.
- Latent heat flux (LE) was flagged (i.e., changed to -999) when LE<-50 W/m^2.
- Sensible heat flux (H) was flagged when H<-70 W/m^2.
- All negative wind speeds were flagged.
- Where LE was flagged and vertical wind speed (w) was >2 or <-2 m/s, w was flagged.
- Where between one and three half-hourly average values of a variable were missing, a linear interpolation was done, assuming that the meteorological conditions were steady and a clear temporal trend was present before and after the data gap.

9.3.2 Calculated Variables

Formulae for the following list of calculated variables can be found in Section 9.1: K*, Ld, Qd, Qu, Q*, Q*corr, a, F_{CO2}, CO_2night, G_total, Ga, Ge, Gveg, G10, SH, and sSH.

9.4 Graphs and Plots

Day 260 in 1996 was chosen because it was a clear day and it shows many interesting contrasting features of the radiation, energy, and CO_2 balances of the two sites (Figure 4). The time shown in the figure is UTC. The most notable differences in the radiation balances between the two sites (Figure 4A and 4B) occur in the net radiation (Q*) and reflected solar radiation (Ku) components: the latter is larger and the former is smaller at the fen as a result of i) the larger albedo at the fen and ii) the higher surface temperatures on the jack pine; which increase the outgoing longwave radiation (Lu) from the drier surface; the greatest contrast in Lu occurs early in the day. The incoming solar radiation (Kd) and incoming longwave radiation (Ld) do not indicate substantial differences between the sites.

The fen had started to senesce by day 260; as a result, the majority of the available energy goes into sensible heat flux (average Bowen ratio 2.0) (Figure 4C). The YJP was still actively transpiring (average Bowen ratio 1.0), except for a short period in the middle of the day when the sensible heat flux exceeds the latent heat flux (Figure 4D). The value of the total heat storage (G_total) includes the soil heat storage and biomass storage from the north site.

The impact of senescence is very noticeable in the different net CO_2 flux patterns. The fen is either effluxing or in a state of zero net exchange for the majority of the day (Figure 4E), but there is some very weak uptake in the late morning. The jack pine shows vigorous uptake for the whole daylight period and consistent efflux in the nighttime period at the start of the day (Figure 4F). The pattern of efflux breaks down late in the day under the very calm wind speed conditions (Figure 4H).

The pattern of wind at the fen is characterized by very low wind speed or complete calm during the night and maximum values of 5 m/s during the daylight period (Figure 4G). The increase of wind speed in the morning and the decrease in the evening are very sharp. The pattern at the YJP is quite different early in the day, when the wind speed increases gradually to a maximum of only 3 m/s by the evening. The precipitous drop in wind speed at 0000 UTC is the same pattern as at the fen. The direction of the wind was steadier at the fen, where it blew from the southeast from 1200 UTC onwards. At the YJP, the direction was more easterly for the majority of the day. It is clear that the fen has its own particular wind climate, and on very calm nights such as the start of day 260, it is much calmer than the more open YJP site (compare Figures 4G and 4H).

The slightly higher and more gradually declining air temperatures at the YJP in the early part of the day (Figure 4H) are consistent with the presence of the higher wind speeds, which would have mixed the lower atmosphere more effectively. The increased mixing would hinder the development of a surface temperature inversion and raise the air temperature. It is important to note that the eddy covariance measurement of CO_2 was very successful at this time of the day, when a constant efflux of 1 µmole/m^2/s was measured (Figure 4F). The same is not true for the fen, where the CO_2 series is quite jagged (Figure 4E) as a result of measured negative fluxes that have been set to zero as part of the data management. Clearly, the measurement of the flux was breaking down at the fen under the totally calm wind speed conditions (Figure 4G).

Figure 4: Radiation, energy, and carbon balances, FEN and YJP sites on DOY 260, 1996.
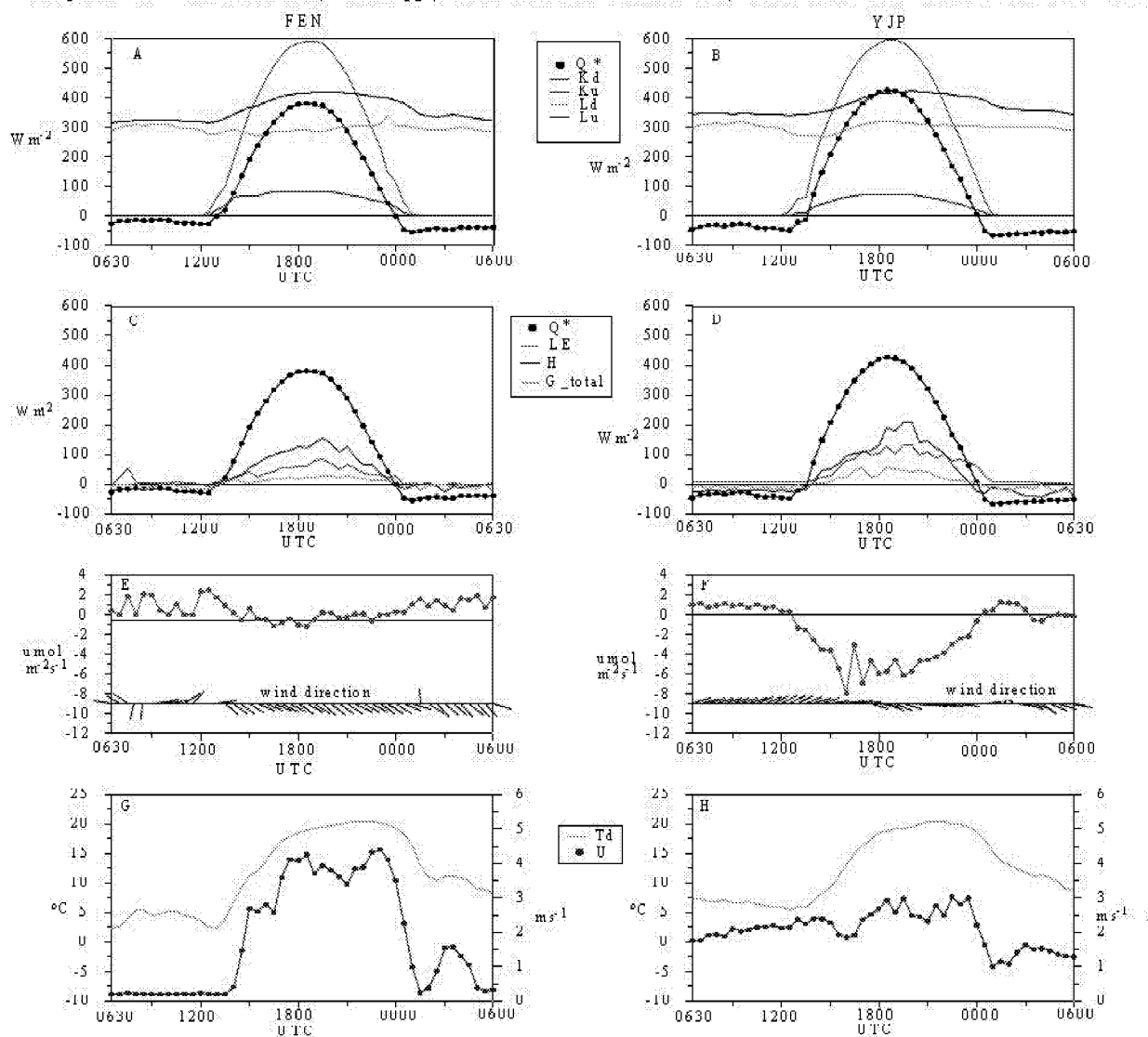
Figure 4: Contrasting Radiation, Energy, and CO$_2$ Balances Between NSA-Fen and NSA-YJP

10. Errors

10.1 Sources of Error

There are a number of sources of error in the data. In general, these sources can be identified as: i) instrument error, i.e., the error component from the transducer itself, ii) a component from the measurement device, and iii) a component dependent upon field placement. Not all of the components of error are easily evaluated, and the most difficult to evaluate through a formal analysis is that due to field placement. We believe that we minimized field placement error, but we do not have a formal way of verifying this claim. We do claim that all instruments were located according to normal field practice, and a close watch was kept by field staff for any apparent aberrant output from the instruments.

10.2 Quality Assessment

All aberrant data occurrences found in the field were noted in the field log and examined in detail during postprocessing. There are a number of reasons for the occurrence of aberrant values. In our particular case, the two most common reasons were i) shutdown of the CO_2 system for calibration, which was done once a day and which resulted in the loss of one 30-minute average value, and ii) covering of the sonic anemometer to prevent its damage by heavy rain. There were various other occurrences of apparently aberrant values unrelated to these two causes. In order to try to identify aberrant behavior more formally, during postprocessing all raw time series were scanned for each day and the outliers from the series were identified and examined in detail. In addition, the calculated time series of fluxes were examined for outliers. Typically, when an outlier was found, the field notes were consulted to see if some action on the tower or in the vicinity of the instrument had been recorded that would have caused the outlier to occur. Irrespective of whether we could tie the outlier to a cause, a simple linear interpolation was applied if the outlier was judged aberrant, the period of bad data was short, and steady-state conditions applied. If it was clear that the data point was wrong and it could not be corrected or interpolated, it was flagged and a missing value place holder inserted. It is admitted that this process is not totally objective and it does involve some judgments based upon field experience. We do claim that the data acceptance criteria were conservative; i.e., it was normal to reject an apparently aberrant data point unless there was very strong evidence to the contrary.

10.2.1 Data Validation by Source

The overall best estimate of accuracy of the primary variables are as follows:

```
net radiation:       ± 5%
PPFD:                ± 7%
solar radiation:     ± 1%
soil heat flux:      ± 5% for YJP; no estimate is made for fen
latent heat flux:    ± 15 to 20%
sensible heat flux:  ± 15 to 20%
CO2 flux             : ± 20% or ± 0.2 umol/m2/s2, whichever is larger
wind speed (model 12102): ± 0.3 m/s from 0 to 30 m/s
wind direction (model 12302): ± 3.0 degrees
air temperature(T/RH sensor, model 41372): ± 0.3 °C from -50 to + 50 °C
relative humidity (T/RH sensor, model 41372): ± 3% between 10 and 90% RH, and
                     ± 5% between 0 and 10% and between 90 and 100% RH
rainfall (model TE525M, Texas Instruments): ± 1% up to 10 mm/h
                                            ± 3% between 10 and 20 mm/h
                                            ± 5% between 20 and 30 mm/h
```

In 1993, 1995, and 1996, no correction factor was applied to the fen's soil heat flux data. Rather, we report the flux values measured by the plate(s). This is a puzzling result, but if the same correction value had been applied as in 1994, totally unreasonable values of flux would have resulted. In fact, the

energy balance closures would have consistently been much greater than unity as a result. This points out the difficulty of measuring heat storage in the peat soil. We suggest that our application of different methodologies can be explained in the following way. In 1994, only the plate in the hollow exhibited any diurnal pattern, but the size and amplitude of the measured flux was tiny. The signal from the plate in the hummock showed zero amplitude, and was a flat line during the whole day, we believe as a result of poor thermal contact between the plate and the peat. Such patterns were not observed in the other sample years, when both plates exhibited similar and significant signal sizes and diurnal amplitudes. Furthermore, accepting the measured fluxes in these sample years results in reasonable energy balance closures. However, the measurement of soil heat flux on a fen remains a confounding problem, and it requires further careful assessment in terms of measurement methodology.

Another problem that caused serious questioning of our methodology was the measurement of the CO_2 flux at night. This problem was most apparent at the YJP. After examination of the data, it was concluded that the measured fluxes should be replaced with modeled values in order to obtain reasonable diurnal patterns. The issue of how best to measure CO_2 fluxes at night under low turbulent mixing conditions remains a priority. In addition, there are outstanding issues on the best way to model the nighttime CO_2 flux.

10.2.2 Confidence Level/Accuracy Judgment
None given.

10.2.3 Measurement Error for Parameters
See Section 10.2.1.

10.2.4 Additional Quality Assessments
None given.

10.2.5 Data Verification by Data Center
Data were examined to check for spikes, values that were four standard deviations from the mean, long periods of constant values, and missing data.

11. Notes

11.1 Limitations of the Data
At this time (June 1998), the data series are not continuous. Where there were measurement problems, e.g., as a result of a sensor failure or a power failure, missing value place holders have been inserted. We are working toward providing robust methods for reconstruction of large data gaps. One method that has been fairly successful is to construct the diurnal patterns of fluxes using ensemble averaging. However, for users who require unbroken time series of 30-minute averages, these data will fall short. In most instances of a small gap, say one or two contiguous half-hours, in a period of steady-state atmospheric conditions, straight linear interpolation should work satisfactorily. If the atmospheric conditions are changing rapidly, or if the gap is large, say half a day, then a rigorous interpolation method will be required. Please consult the PI for progress on the development of interpolation routines for large data gaps.

At this time (June 1998), the eddy covariance flux data (sensible and latent heat and CO_2) at the YJP site are from the Campbell Scientific single-axis sonic anemometer. A second sonic anemometer (Applied Technologies, Inc., (ATI), Boulder, CO, USA) was operational at the site in 1996, and both were located at the same height and orientation on the flux tower. The final calculation of the fluxes based on the ATI sonic data are not yet complete and are not included in this data set.

11.2 Known Problems with the Data

Where tower flux sites do not have adequate upwind fetch, uncertainties are introduced into the interpretation of the flux data. We believe this may have been a problem at the fen. The eddy covariance instruments were located at a height of 4.5 m above the surface. Using the standard micrometeorological "rule-of-thumb" for fetch-to-height ratio of 100:1, a 4500-m fetch is required in all directions around the fen tower. The site did not meet this criterion. Fetch was limited along the northeast shore in the azimuth directions (from magnetic north) 350-0-125 degrees. Minimum fetch in this quadrant was approximately 150 m at a bearing 65 degrees. Similarly, fetch was limited along the south shore in the bearing 160-235 degrees. Minimum fetch in this quadrant was 220 m at the bearing 205 degrees. Fetch in all other directions exceeded 450 m. Measurements for all wind directions were reported in the data set, and users are cautioned as to this possible source of uncertainty.

Fetch to height ratios at YJP were greater than 100:1 in all directions. However, the sector azimuth 45-140 degrees contains the access trail to the tower, the instrument and data processing hut, and the generator hut. Some contamination of fluxes measured from this direction may have occurred.

11.3 Usage Guidance

In 1994 at YJP, recording of the deep soil temperatures (0.25, 0.50, and 0.75 m) at the north soil heat flux site did not start until DOY 179 1994. This contrasts to the measurements at the west site, where recording began on DOY 144. As a result, lower minimum deep soil temperature values were observed at the west site. This phenomenon is reflected in the max/min summary in Section 7.3.5..

In the modeled nighttime carbon dioxide flux series, all negative values (uptake) were kept in the data set because there was no rationale for removing them. They occurred as a result of the nature of the empirical model (equation 9.11) used for the estimate.

11.4 Other Relevant Information

None.

12. Application of the Data Set

These data can be used for various applications. For example, they will provide meteorological input variables for a wide range of models. Also, for those models that estimate fluxes, the data set provides flux data series for sensible and latent heat and CO_2 for model verification.

13. Future Modifications and Plans

Once the data processing is complete, we will submit the convective and CO_2 flux data for YJP in 1996 based on measurements from the ATI sonic. Secondly, we are working on a more objective method to fill data gaps. To date, we have used linear interpolation. This method applies only to short periods, a few half-hours at best, under steady-state conditions. If the meteorological conditions are changing, linear interpolation fails. It also fails if the data gap is longer than a few half-hours. When we encountered a long data gap, we have left the data field blank and assigned a "missing value" place holder. Given that we did have significant gaps in the flux series because of the difficulties of the Campbell sonic in rainy weather, we have used ensemble averaging to create complete average diurnal curves of fluxes for publications. We recognize that ensemble average data are not necessarily the ideal kind for modelers who prefer unbroken time series for each variable.

14. Software

14.1 Software Description
The measurement of the raw data was principally on Campbell Scientific data loggers, and all of the specific control programs for these data loggers are available.

A variety of software was used in the data assessment and analysis. STORAG, a Fortran program to find the minor heat storage terms in the energy balance, calculated the surface soil heat flux, the biomass heat storage, and the latent and sensible heat storage in the air up to the level of measurement of net radiation, where the surface balance was closed. RADBAL, a Fortran program to solve the terms of the energy balance, was used in the analysis of the radiation balance data, including the calculation of shortwave and PPFD albedos, and the radiative surface temperatures. We developed a number of QuattroPro spreadsheets for the calculation of convective fluxes (H and LE) and the CO_2 flux, including the correction of the fluxes for density effects and ensemble averaging to construct average daily flux patterns for the days included in the average. Ensemble averaging was used as a means to find the mean diurnal pattern from often incomplete flux data series on individual days. This methodology was successful and was favored over the development of other means for filling data gaps. However, active research on the issue of how best to fill data gaps continues.

14.2 Software Access
All software developed for the analysis of the data is available by contacting J.H. McCaughey (PI).

15. Data Access

The NSA-YJP tower flux, meteorological, and porometry data are available from the Earth Observing System Data and Information System (EOSDIS) Oak Ridge National Laboratory (ORNL) Distributed Active Archive Center (DAAC).

15.1 Contact Information
For BOREAS data and documentation please contact:

ORNL DAAC User Services
Oak Ridge National Laboratory
P.O. Box 2008 MS-6407
Oak Ridge, TN 37831-6407
Phone: (423) 241-3952
Fax: (423) 574-4665
E-mail: ornldaac@ornl.gov or ornl@eos.nasa.gov

15.2 Data Center Identification
Earth Observing System Data and Information System (EOSDIS) Oak Ridge National Laboratory (ORNL) Distributed Active Archive Center (DAAC) for Biogeochemical Dynamics
http://www-eosdis.ornl.gov/.

15.3 Procedures for Obtaining Data
Users may obtain data directly through the ORNL DAAC online search and order system [http://www-eosdis.ornl.gov/] and the anonymous FTP site [ftp://www-eosdis.ornl.gov/data/] or by contacting User Services by electronic mail, telephone, fax, letter, or personal visit using the contact information in Section 15.1.

15.4 Data Center Status/Plans
The ORNL DAAC is the primary source for BOREAS field measurement, image, GIS, and hardcopy data products. The BOREAS CD-ROM and data referenced or listed in inventories on the CD-ROM are available from the ORNL DAAC.

16. Output Products and Availability

16.1 Tape Products
None.

16.2 Film Products
None.

16.3 Other Products
These data are available on the BOREAS CD-ROM series.

17. References

17.1 Platform/Sensor/Instrument/Data Processing Documentation
All persons from Queen's University, Kingston, Ontario, who worked on the flux towers received training on tower climbing techniques, tower rescue methods, and the operation of a safe field site. The material is summarized in McCaughey (1993), and a summary of the training materials can be found in the tower safety document.

The data analysis to find the minor heat storage terms in the energy balance was accomplished with the software program titled STORAG, and details of this software are available in McCaughey (1991).

17.2 Journal Articles and Study Reports

Alemdag, I.S. 1983. Mass equations and merchantability factors for Ontario softwoods. Inf. Rep. PI-X-23, 27, Natl. For. Inst., Petawawa, Ontario, Canada.

Brand, D.G. 1987. Estimating the surface area of spruce and pine foliage from displaced volume and length. Can. J. For. Res. 17:1305-1308.

Campbell, G.S. and B.D. Tanner. 1985. A krypton hygrometer for measurement of atmospheric water vapor concentration. Moisture and Humidity 1985, Measurement and Control in Science and Industry, Proc. 1985 Intl. Symp. on Moisture and Humidity, Washington, DC, 609-612.

Campbell, G.S. and M.H. Unsworth. 1979. An inexpensive sonic anemometer for eddy correlation. J. Appl. Meteorol. 18:1072-1077.
Chen, J.M. and T.A. Black. 1992. Foliage area and architecture of plant canopies from sunfleck size distributions. Agric. For. Meteorol. 60:249-266.

Costello, A.M. 1995. Canopy Characteristics and Surface-Atmosphere Interactions of a Young Jack Pine Forest Near Thompson, Manitoba, M.Sc. Thesis, Queen's University, Kingston, Ontario, 125 pp.

Gower, S.T. and J.M. Norman. 1991. Rapid estimation of leaf area index in conifer and broad-leaf plantations. Ecology 72:1896-1900.

Halliwell, D.H. and W.R. Rouse. 1987. Soil heat flux in permafrost: Characteristics and accuracy of measurement. J. Climatol. 7:571-584.

Hodges, G.B. and E.A. Smith. 1997. Intercalibration, objective analysis, inter-comparison and synthesis of BOREAS surface net radiation measurements. Journal of Geophysical Research 102(D24): 28,885-28,900.

Joiner, D.W. 1994. Corrections to TF-10 eddy covariance fluxes. Queen's University internal report, 23 pp.

Lafleur, P.M., J.H. McCaughey, D.W. Joiner, P.A. Bartlett, and D.E. Jelinski. 1997. Seasonal trends in energy, water, and carbon dioxide fluxes at a northern boreal wetland. Journal of Geophysical Research 102(D24): 29,009-29,020.

Leclerc, M.Y. and G.W. Thurtell. 1990. Footprint prediction of scalar fluxes using a Markovian analysis. Boundary-Layer Meteorol. 52:247-258.

Leuning, R. and J. Moncrieff. 1990. Eddy-covariance CO_2 flux measurement using open- and closed-path CO_2 analyzers: Corrections for analyzer water vapor sensitivity and damping of fluctuations in air sampling tubes. Boundary-Layer Meteorol. 53:63-76.

Leuning, R. and K.M. King. 1992. Comparison of eddy-covariance measurements of CO_2 fluxes by open- and closed-path CO_2 analyzers. Boundary-Layer Meteorol. 59:297-311.

McCaughey, J.H. 1991. Safety in Climatology: a Seminar on Tower Climbing. 7 pp., 1987, last revision in 1993.

McCaughey, J.H. RTDMS Program Manual, Second Edition, Delta T Documents, 50 pp.

McCaughey, J.H. and W.L. Saxton. 1988. Energy balance storage terms in a mixed forest. Agric. For. Meteorol. 44:1-18.

McCaughey, J.H., P.M. Lafleur, D.W. Joiner, P.A. Bartlett, A.M. Costello, D.E. Jelinski, and M.G. Ryan. 1997. Magnitudes and seasonal patterns of energy, water, and carbon exchanges at a boreal young jack pine forest in the BOREAS northern study area. Journal of Geophysical Research 102(D24): 28,997-29,007.

Mueller-Dombois, D. and H. Ellenberg. 1974. Aims and Methods of Vegetation Ecology. J. Wiley & Sons, New York, 547 pp.

Newcomer, J., D. Landis, S. Conrad, S. Curd, K. Huemmrich, D. Knapp, A. Morrell, J. Nickeson, A. Papagno, D. Rinker, R. Strub, T. Twine, F. Hall, and P. Sellers, eds. 2000. Collected Data of The Boreal Ecosystem-Atmosphere Study. NASA. CD-ROM.

Saxton, W.L. and J.H. McCaughey. 1988. Measurement considerations and trends in biomass heat storage of a mixed forest. Can. J. For. Res. 18:143-149.

Schmid, H.P. and T.R. Oke. 1990. A model to estimate the source area contributing to turbulent exchange in the surface layer over patchy terrain. Quart. J. Roy. Meteorol. Soc. 116:965-988.

Sellers, P. and F. Hall. 1994. Boreal Ecosystem-Atmosphere Study: Experiment Plan. Version 1994-3.0, NASA BOREAS Report (EXPLAN 94).

Sellers, P. and F. Hall. 1996. Boreal Ecosystem-Atmosphere Study: Experiment Plan. Version 1996-2.0, NASA BOREAS Report (EXPLAN 96).

Sellers, P., F. Hall, and K.F. Huemmrich. 1996. Boreal Ecosystem-Atmosphere Study: 1994 Operations. NASA BOREAS Report (OPS DOC 94).

Sellers, P., F. Hall, and K.F. Huemmrich. 1997. Boreal Ecosystem-Atmosphere Study: 1996 Operations. NASA BOREAS Report (OPS DOC 96).

Sellers, P., F. Hall, H. Margolis, B. Kelly, D. Baldocchi, G. den Hartog, J. Cihlar, M.G. Ryan, B. Goodison, P. Crill, K.J. Ranson, D. Lettenmaier, and D.E. Wickland. 1995. The boreal ecosystem-atmosphere study (BOREAS): an overview and early results from the 1994 field year. Bulletin of the American Meteorological Society. 76(9):1549-1577.

Sellers, P.J., F.G. Hall, R.D. Kelly, A. Black, D. Baldocchi, J. Berry, M. Ryan, K.J. Ranson, P.M. Crill, D.P. Lettenmaier, H. Margolis, J. Cihlar, J. Newcomer, D. Fitzjarrald, P.G. Jarvis, S.T. Gower, D. Halliwell, D. Williams, B. Goodison, D.E. Wickland, and F.E. Guertin. 1997. BOREAS in 1997: Experiment Overview, Scientific Results and Future Directions. Journal of Geophysical Research 102(D24): 28,731-28,770.

Smith, E.A., G.B. Hodges, M. Bacrania, H.J. Cooper, M.A. Owens, R. Chappell, and W. Kincannon. 1997. Final Report NASA Grant NAG5-2447, BOREAS Net Radiometer Engineering Study. Goddard Space Flight Center, Greenbelt, Maryland. 51 pp.

Smith, N.J., J.M. Chen, and T.A. Black. 1993. Effects of clumping on estimates of stand leaf area index using the LI-COR LAI 2000. Can. J. For. Res. 23:1940-1943.

Tanner, B.T., E. Swiatek, and J.P. Greene. 1993. Density fluctuations and use of the krypton hygrometer in surface flux measurements. Proceedings of the 1993 National Conference on Irrigation and Drainage Engineering, American Society of Civil Engineers, Park City, Utah.

Thom, A.S. 1975. Momentum, mass and heat exchange of plant communities. In: Vegetation and the Atmosphere, Vol. 1 (Ed. J. L. Monteith), Academic Press, London. pp. 57-109.

Webb, E.K. 1982. On the correction of flux measurements for effects of heat and water vapor transfer. Boundary-Layer Meteorol. 23:251-254.

Webb, E.K., G.I. Pearman, and R. Leuning. 1980. Correction of flux measurements for density effects due to heat and water vapor transfer. Quart. J. Roy. Meteorol. Soc. 106:85-100.

17.3 Archive/DBMS Usage Documentation
None.

18. Glossary of Terms

Symbol	Quantity	Units
a	Albedo	dim.
AT	Total needle area	cm2
C	Volumetric heat capacity of soil	J/m3/°C
C'	CO2 concentration per volume fluctuation	ppmv
CF	Correction factor	dim.
Cm	Heat capacity of mineral fraction	J/m3/°C
Co	Heat capacity of organic soil	J/m3/°C
CO2night	Net CO2 flux from model when Kd<5 W/m2	μmol/m2/s
CON	Constant used in STORAG to find heat storage in air, soil, and vegetation	J/m3/°C/s
Cp	Specific heat of air at constant pressure	J/kg/°C
Cw	Heat capacity of water	J/m3/°C
dbh	Diameter at breast height	cm
de	Rate of change in vapor pressure	kPa/s
dim.	Dimensionless number	dim.

DS	Depth of temperature measurements	m
dTa	Rate of change in air temperature	°C/s
dTb	Rate of change in biomass temperature	°C/s
dTs	Rate of change in soil temperature	°C/s
FeCO2	Eddy flux of CO2 (equivalent to net flux at height of measurement)	µmol/m2/s or mg/m2/s
FsCO2	Storage flux of CO2	µmol/m2/s
FCO2	Total CO2 flux	µmol/m2/s
G	Soil heat flux at surface	W/m2
G(z)	Soil heat flux measured at depth z	W/m2
G10	Heat storage in the soil volume above 10-cm depth	W/m2
Ga	Sensible heat storage in air	W/m2
GB	Heat flux out the bottom of the soil profile at the fen	W/m2
Gcal	Total heat storage in the soil profile at fen	W/m2
Ge	Latent heat storage in air	W/m2
Gfen	Ground heat flux at the fen in 1994	W/m2
Ghol	Ground heat flux in hollow at the fen	W/m2
G(z)n	Soil heat flux at YJP (north site)	W/m2
Gpla	Time-integrated soil flux from plate at fen	W/m2
G(z)w	Soil heat flux at YJP (west site)	W/m2
G_total	Total heat storage	W/m2
G_totaln	Total heat storage at YJP (north site)	W/m2
G_totalw	Total heat storage at YJP (west site)	W/m2
Gveg	Heat storage in biomass at YJP	W/m2
Gvegn	Heat storage in biomass at YJP (north site)	W/m2
Gvegw	Heat storage in biomass at YJP (west site)	W/m2
h	Tree height	m
H	Sensible heat flux	W/m2
HCS	Heat capacity of soil in STORAG	J/m3/°C
Kd	Incoming solar radiation	W/m2
Ku	Reflected solar radiation	W/m2
Ks	Thermal conductivity of saturated peat soil	W/m/K
k	Instrument H2O vapor absorption coefficient	m3/kg/cm
K*	Total shortwave radiation	W/m2
L	Latent heat of vaporization of water	J/kg
LE	Latent heat flux	W/m2
Ld	Incoming longwave radiation	W/m2
Lu	Outgoing longwave radiation	W/m2
L*	Net longwave radiation	W/m2
M	Molecular weight of dry air	Mole
mis.	Missing value	dim.
Mv	Standing green biomass	kg/m2
P	Atmospheric pressure	kPa
PA	Total projected needle area	cm2
PA(S)	Shoot projected area	cm2
PPFDd	Incoming PPFD	µmol/m2/s
PPFDu	Reflected PPFD	µmol/m2/s
Qd	Total incoming radiation	W/m2
QGZ	Soil heat flux from flux plate (for STORAG only)	W/m2
Qu	Total outgoing radiation	W/m2
Q*	Net radiation	W/m2
Q*corr	Corrected net radiation (following Hodges and Smith (1997))	W/m2

```
q              Water vapor density                              g/m3
q'             Water vapor density fluctuation                  g/m3
R              Universal gas constant                           J/mol/K
R'             Conifer correction factor                        dim.
rho            Density of air                                   kg/m3
rho(c)         Density of CO2                                   kg/m3
s              Signal voltage from hygrometer                   mv
S              Flux equivalent to the heat stored between       W/m2
                 individual soil layers
SH             Specific humidity                                g/kg
sSH            Standard deviation of specific humidity          g/kg
T'             Temperature fluctuation                          °C
T_air          Air temperature                                  °C
TB             Biomass temperature in STORAG                    °C
Tblw           Stem temperature of large trees (west site)      °C
Tbmw           Stem temperature of medium trees (west site)     °C
Tbsn           Stem temperature of small trees (north site)     °C
Tbsw           Stem temperature of small trees (west site)      °C
TD             Dry bulb temperature in STORAG                   °C
TOL            Thickness of organic layer in STORAG             m
Ts             Soil temperature                                 °C
Ts10avg        Average soil temperature at 10-cm depth          °C
Ts75avg        Average soil temperature at 75-cm depth          °C
TW             Wet-bulb temperature                             °C
U              Wind speed                                       m/s
v              Intercept of the krypton hygrometer calibration  mv
w'             Vertical wind velocity                           m/s
x              Path length of the hygrometer                    cm
Xm             Soil volumetric mineral fraction                 fraction
Xo             Soil volumetric organic soil fraction            fraction
Xw             Soil volumetric water fraction                   fraction
XW             Soil moisture content in STORAG                  fraction
z              Depth to soil heat flux plate                    m
ZCQ            Control variable in STORAG; used to read two     m,m
                 variables: height of canopy and heightof net
                 pyrradiometer
zr             Reference height                                 m
ZR             Height of net radiation measurement in early     m
                 version of STORAG
```

19. List of Acronyms

```
AES     Atmospheric Environment Services
AFM     Airborne Fluxes and Meteorology
ASCII   American Standard Code for Information Interchange
ATI     Applied Technologies, Inc.
BOREAS  BOReal Ecosystem-Atmosphere Study
BORIS   BOREAS Information System
CCRS    Canada Centre for Remote Sensing
CD-ROM  Compact Disk-Read-Only Memory
CGR     Certified by Group
CO2     Carbon dioxide
CPI     Certified by PI
```

```
CPI-??? Certified but questionable
DAAC    Distributed Active Archive Center
DC      Direct Current
DOY     Day of Year
ENBAL   Energy Balance (analysis program)
EOS     Earth Observing System
EOSDIS  EOS Data and Information System
Fen     Fen wetland site
FFC     Focused Field Campaign
FPAR    Fraction of PPFD absorbed by the vegetation canopy
GIS     Geographic Information System
GMT     Greenwich Mean Time
GPS     Global Positioning System
GSFC    Goddard Space Flight Center
HTML    HyperText Markup Language
HYD     Hydrology
IRGA    Infrared Gas Analyzer
LAI     Leaf Area Index
LW      Longwave
MV      Mass of Vegetation
N/A     Not available
NAD83   North American Datum of 1983
NARC    National Atmospheric Radiation Center
NASA    National Aeronautics and Space Administration
NEE     Net Ecosystem Exchange
NOAA    National Oceanic and Atmospheric Administration
NSA     Northern Study Area
ORNL    Oak Ridge National Laboratory
PANP    Prince Albert National Park
PAR     Photosynthetically Active Radiation
PCQM    Point Center Quarter Method
PNFI    Petawawa National Forest Institute
PPFD    Photosynthetic Photon Flux Density
RADBAL  Radiation Balance (analysis program)
REBS    Radiation Energy Balance Systems, Inc.
RH      Relative humidity
RSS     Remote Sensing Science
SB      Short, below breast height
SCF     Shoot Clumping Factor
SRC     Saskatchewan Research Council
STORAG  (heat) storage (analysis program)
SVAT    Soil-Vegetation-Atmosphere-Transfer
SW      Shortwave
TA      Tall, above breast height
TB      Tall, below breast height
TF-10   Tower Flux group 10
URL     Uniform Resource Locator
UTC     Universal Time Coordinated
UTM     Universal Transverse Mercator
WAB     Wind Aligned Blob
WPL     Webb, Pearman, and Leuning flux correction
YJP     Young Jack Pine forest site
```

20. Document Information

20.1 Document Revision Date
Written: 06-Jun-1998
Revised: 28-Sep-1999

20.2 Document Review Date(s)
BORIS Review: 25-Apr-1999
Science Review:

20.3 Document ID

20.4 Citation
When using these data, please include the following acknowledgment as well as citations of relevant papers in Section 17.2:

These data were provided by BOREAS Team TF-10; the primary consultants include:

Flux and meteorological data (YJP and Fen):
Dr. J. Harry McCaughey, Department of Geography, Queen's University, Kingston, ON, CANADA, K7L 3N6 (PI) and Dr. Peter M. Lafleur, Department of Geography, Trent University, Peterborough, ON, CANADA, K9J 7B8. Both investigators should be acknowledged in all future publications.

Fen biophysical data:
Dr. D.E. Jelinski, Department of Geography, Queen's University, Kingston, ON, CANADA, K7L 3N6 (PI).

YJP biophysical data:
Dr. J. Harry McCaughey, Department of Geography, Queen's University, Kingston, ON, CANADA, K7L 3N6 (PI).

If using data from the BOREAS CD-ROM series, also reference the data as:
McCaughey, J.H. and D.E. Jelinski, "Surface Energy and Water Balances of Forest and Wetland Subsystems in the Boreal Forest - Surface Atmosphere Links and Ecological Controls." In Collected Data of The Boreal Ecosystem-Atmosphere Study. Eds. J. Newcomer, D. Landis, S. Conrad, S. Curd, K. Huemmrich, D. Knapp, A. Morrell, J. Nickeson, A. Papagno, D. Rinker, R. Strub, T. Twine, F. Hall, and P. Sellers. CD-ROM. NASA, 2000.

Also, cite the BOREAS CD-ROM set as:
Newcomer, J., D. Landis, S. Conrad, S. Curd, K. Huemmrich, D. Knapp, A. Morrell, J. Nickeson, A. Papagno, D. Rinker, R. Strub, T. Twine, F. Hall, and P. Sellers, eds. Collected Data of The Boreal Ecosystem-Atmosphere Study. NASA. CD-ROM. NASA, 2000.

20.5 Document Curator

20.6 Document URL

REPORT DOCUMENTATION PAGE

Public reporting burden for this collection of information is estimated to average 1 hour per response, including the time for reviewing instructions, searching existing data sources, gathering and maintaining the data needed, and completing and reviewing the collection of information. Send comments regarding this burden estimate or any other aspect of this collection of information, including suggestions for reducing this burden, to Washington Headquarters Services, Directorate for Information Operations and Reports, 1215 Jefferson Davis Highway, Suite 1204, Arlington, VA 22202-4302, and to the Office of Management and Budget, Paperwork Reduction Project (0704-0188), Washington, DC 20503.

1. AGENCY USE ONLY *(Leave blank)*	2. REPORT DATE November 2000	3. REPORT TYPE AND DATES COVERED Technical Memorandum

4. TITLE AND SUBTITLE

Technical Report Series on the Boreal Ecosystem-Atmosphere Study (BOREAS)

BOREAS TF-10 NSA-YJP Tower Flux, Meteorological, and Porometry Data

5. FUNDING NUMBERS

923

RTOP: 923-462-33-01

6. AUTHOR(S)

J. Harry McCaughey and Laura Liblik

Forrest G. Hall and Karl Huemmrich, Editors

7. PERFORMING ORGANIZATION NAME(S) AND ADDRESS (ES)

Goddard Space Flight Center
Greenbelt, Maryland 20771

8. PEFORMING ORGANIZATION REPORT NUMBER

2000-03136-0

9. SPONSORING / MONITORING AGENCY NAME(S) AND ADDRESS (ES)

National Aeronautics and Space Administration
Washington, DC 20546-0001

10. SPONSORING / MONITORING AGENCY REPORT NUMBER

TM—2000–209891
Vol. 208

11. SUPPLEMENTARY NOTES

J.H. McCaughey and L. Liblik: Queen's University, Kingston, Ontario;
K. Huemmrich: University of Maryland, NASA Goddard Space Flight Center, Greenbelt, Maryland

12a. DISTRIBUTION / AVAILABILITY STATEMENT

Unclassified–Unlimited
Subject Category: 43
Report available from the NASA Center for AeroSpace Information,
7121 Standard Drive, Hanover, MD 21076-1320. (301) 621-0390.

12b. DISTRIBUTION CODE

13. ABSTRACT *(Maximum 200 words)*

The BOREAS TF-10 team collected tower flux and meteorological data at two sites, a fen and a young jack pine forest, near Thompson, Manitoba, Canada, as part of BOREAS. A preliminary data set was assembled in August 1993 while field testing the instrument packages, and at both sites data were collected from 15-Aug to 31-Aug. The main experimental period was in 1994, when continuous data were collected from the young jack pine site from 23-May to 20-Sep. Upon examination of the 1994 data set, it became clear that the behavior of the heat, water, and carbon dioxide fluxes throughout the whole growing season was an important scientific question, and that the 1994 data record was not sufficiently long to capture the character of the seasonal behavior of the fluxes. Thus, the young jack pine site was operated from 08-May to 07-Nov in 1996 in order to collect data from spring melt to autumn freeze-up. All variables are presented as 30-minute averages. Supporting data were also collected to describe the surface's state and to provide the information, in association with the flux data, to build SVAT models. For the young jack pine site, these supporting data included stomatal conductance measurements. The data are stored in tabular ASCII files.

14. SUBJECT TERMS

BOREAS, tower flux, meteorological data, porometry data.

15. NUMBER OF PAGES

66

16. PRICE CODE

17. SECURITY CLASSIFICATION OF REPORT Unclassified	18. SECURITY CLASSIFICATION OF THIS PAGE Unclassified	19. SECURITY CLASSIFICATION OF ABSTRACT Unclassified	20. LIMITATION OF ABSTRACT UL